# Compound Weather Extreme Events and Their Impacts: Towards a Better Understanding of Compound Events

Catastrophe and Climate

NOVEMBER | 2024

SOA Research INSTITUTE
SOCIETAL PURPOSE

# Compound Weather Extreme Events and their Impacts

## Towards a better understanding of compound events

**AUTHORS** AXA Climate research team:
Christelle Castet
Antoine Guy
Sophie Abramian
Derek Wu

**SPONSOR** Catastrophe and Climate Strategic Research Program Steering Committee

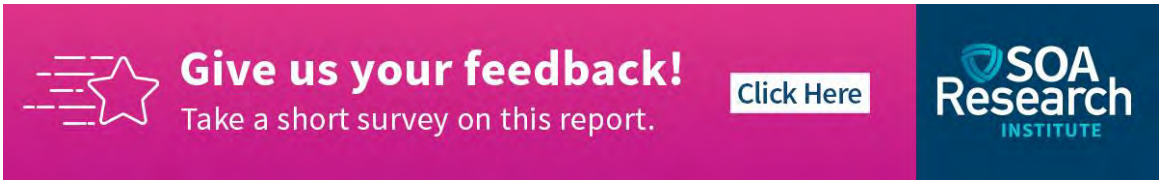

# CONTENTS

# Compound Weather Extreme Events and their Impacts

## Towards a better understanding of compound events

## Executive Summary

Originally introduced by the Intergovernmental Panel on Climate Change (IPCC) in 2012, research on compound events, defined as *combinations of multiple drivers and hazards that contribute to societal or environmental risk*s, has grown with the goal to understand how different weather and climate-related hazards interact, hence improving prediction, assessing impacts on society and the environment, and developing methods for detection and attribution.

Three typologies of compound events (see Figure 1.0 below) are studied in this research to investigate how they would affect the frequency and the severity of various impacts or effects to climatic activities, summarized in Table 1 below:

Table 1
TYPES OF COMPOUND EVENTS

| Compound Events | Definition and Research Scope | Impacts/ Effects |
|---|---|---|
| **Temporally compounding event** | This refers to a succession of hazards that affect a given geographical region.<br><br>This study looks at positive temperature anomalies and drought hazards with a 1-month lag and explores how they affect the risk of wildfire in California. | Our study concluded that wildfires are 62% and 26% more likely to happen during a temporally compounding event than during a non-compounded drought and heat event, respectively.<br><br>When differentiating the wildfire season against the rest of the year, compound events increase the risk both during and outside the wildfire season. The risk increase outside the wildfire season is 71% and 56% higher for a compounding event when compared to a non-compounded drought and heat event, respectively. During the wildfire season, there is a 75% increase in frequency for a compound event compared to a drought event (22% increase compared to heat event). |
| **Multivariate compounding event** | This refers to the co-occurrence of multiple climate drivers and/or hazards in the same geographical region causing an impact.<br><br>This study looks at the effect on the yield of the co-occurrence of drought and positive temperature | When investigating on the effect on crop yield, we found that there is a 70% risk of having a yield below the mean when dealing with a compound event versus 50% risk for non-compound events. In a compound event, a median yield of -7% below the average is observed compared to +2% and +3% for drought and heat events, respectively. |

| | | |
|---|---|---|
| | anomalies during the flowering period of wheat. | |
| **Spatially compounding event** | This occurs when multiple connected locations are affected by the same hazard within a limited time window.<br><br>This study focuses on the role played by El Niño–Southern Oscillation (ENSO) and Atlantic Multidecadal Oscillation (AMO), two modulators of sea surface temperature in the Pacific and Atlantic, with tropical cyclone activity. | Globally, the two climate modulators of AMO and ENSO do not observe a coherent trend across basins, but appear to have opposite impacts on the North Atlantic and Pacific basins::<br>- **ENSO Niño 3.4 index** has a strong positive correlation to both the frequency and intensity of tropical cyclones in the West Pacific and East Pacific basins, indicating more active cyclone seasons during El Niño. In the North Atlantic, the Niño 3.4 index is negatively correlated with cyclone frequency and intensity, reflecting La Niña's influence on heightened cyclone activity. In the Southern Hemisphere, tropical cyclone activity in the South Pacific is positively correlated with ENSO, while the South Indian Ocean basin is negatively correlated with Niño 3.4, likely due to changes in the Walker circulation. The activity in the North Indian Ocean basin shows no significant correlation with ENSO, suggesting other climate modulators, such as the Indian Ocean Dipole, may play a role.<br>- **AMO** is positively correlated with the tropical cyclone frequency over the Atlantic Ocean. Warmer sea surface temperatures associated with the current positive phase of the AMO enhance the formation and intensification of tropical cyclones (hurricanes) in the Atlantic. On the other hand, the AMO is negatively correlated with the tropical cyclone activity over the West Pacific, East Pacific, and South Pacific basins. The positive phase of the AMO has been linked to warming in the subtropical North Pacific, causing atmospheric changes in the tropical Pacific region, including a strengthening of the Walker Circulation and an associated increase in vertical wind shear. |

Going forward, the future warming climate will influence compound events. For instance, based on projections of the future climate over California for the 2050 timeframe (2035-2065) following a "high end" emission scenario named SSP5-8.5 (IPCC 2021), our study suggests there will be a 9% point increase in compound event risk (of positive temperature anomaly and drought). However, the consequent impacts of compound events prove to be more difficult to project without wildfire or crop models, hence a qualitative approach has been taken to shed some light on how climate change affects the impacts:

- For **wildfires**, as there is a large increase in positive temperature anomaly, in general, and even more in the July-November time period, we can expect a longer wildfire season in the western U.S. that would start earlier, intensify in the summer compared to historic experience, but also last longer in autumn.

- For **crop yield**, the trend is not as evident as farmers are likely to adapt their agriculture practices by planting earlier or later according to the changing climate, switching to a more-resilient crop, growing a more robust variety of plants with traits that can resist the changing climate, etc.
- For **tropical cyclone** activity, climate change has many types of impacts on it. There is a strong consensus that an increase in tropical cyclone intensity related to warmer ocean temperatures will lead to stronger and more destructive events. The evolution of the frequency of these events is more uncertain, with studies suggesting a global decrease in frequency, but an increase in the proportion of very intense tropical cyclones. As the atmosphere warms, its water vapor holding capacity increases (Clausius-Clapeyron relation) leading to more intense precipitation and, as sea level rises, storm surge will lead to more extensive flooding.

Figure 1.0
KEY ELEMENTS FOR 3 TYPES OF COMPOUND EVENTS WITH EXAMPLES

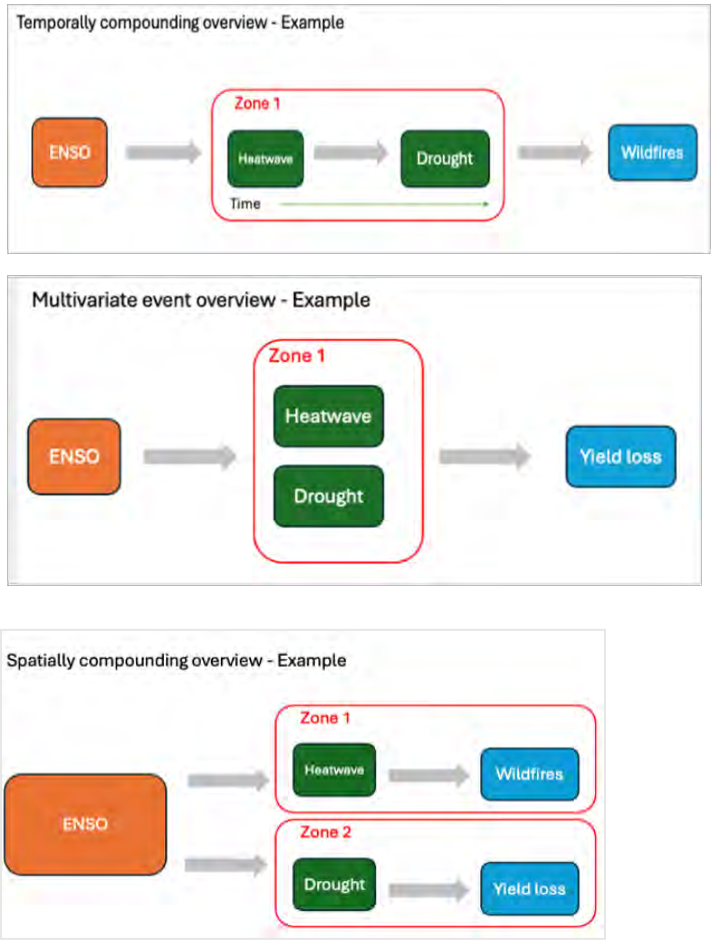

# Section 1: Introduction

## 1.1 CONTEXT AND DEFINITIONS

Climate change is characterized by an increase in the average global temperature and a rise in many types of extreme weather events (IPCC AR6 WGI, 2021; Stott, P. 2016). For instance, heatwaves, droughts, heavy precipitation, and frost periods are expected to become more frequent and more intense (Tripathy, 2023; Fuhrer, J., 2006). This has at least two consequences: firstly, it is increasingly likely that these extreme events will compound, occur in the same location and/or at the same time or successively; secondly, human activities will be more exposed to each of these risks. Studying extremes is challenging because they are, by definition, rare, and studying compound extremes is even more so. Significant research efforts have defined a framework, specifically a typology, for these events. Before delving into the details, it is useful to pose some basic yet fundamental definitions of compound events.

Compound weather events - Originally introduced by the Intergovernmental Panel on Climate Change (IPCC) in 2012, research on compound events—also known as correlated or complex extremes—has grown to involve multiple fields, such as climate science, impact assessment, engineering, and statistics. The goal of this interdisciplinary research is to understand how different weather and climate-related hazards interact, with the aim of improving prediction, assessing impacts on society and the environment, and developing methods for detection and attribution. The definition of compound events has evolved from its initial description in the IPCC's Special Report on Climate Extremes and is now integrated into the IPCC's risk framework as *combinations of multiple drivers and hazards that contribute to societal or environmental risks*. A recent review article from Zscheischler *et al.* (2020) defined the terms modulator, driver, hazard, and impact to help in understanding how climate systems and changes affect the environment and society:

1. Modulator: A modulator refers to factors that can influence or alter the behavior of climate variables over time. These can include natural phenomena like oceanic and atmospheric patterns (e.g., the El Niño-Southern Oscillation) that modulate temperature and precipitation, affecting the climate's variability and intensity.

2. Driver: A driver is a weather process that directly influences climate conditions. It could be a weather system such as a severe storm, a tropical cyclone, a cold front and a stationary high-pressure system.

3. Hazard: A hazard is a potentially damaging climate-related phenomenon resulting from climate drivers. Examples include extreme weather events such as floods, droughts, and heatwaves. Hazards are the direct cause of impacts and, therefore, pose risks to human life, property, and the environment.

4. Impact: Impact refers to the effects of climate hazards on natural and human systems. These can include damage to infrastructure, loss of biodiversity, economic losses, and health effects. Impacts depend on the exposure and vulnerability of systems to the hazards, and they can be detrimental, beneficial, or neutral depending on the context.

In summary, climate drivers are linked to the Earth's atmospheric circulation and regulation processes and can give rise to hazards. These hazards can, in turn, negatively impact infrastructures, crops or human life (as illustrated in Figure 1.1). A climatic driver itself is not the danger, but rather its ability to trigger hazards, which is also linked to the concept of vulnerability (Zscheischler, J. ,2020).

Figure 1.1
ELEMENTS OF COMPOUND WEATHER AND CLIMATE EVENTS

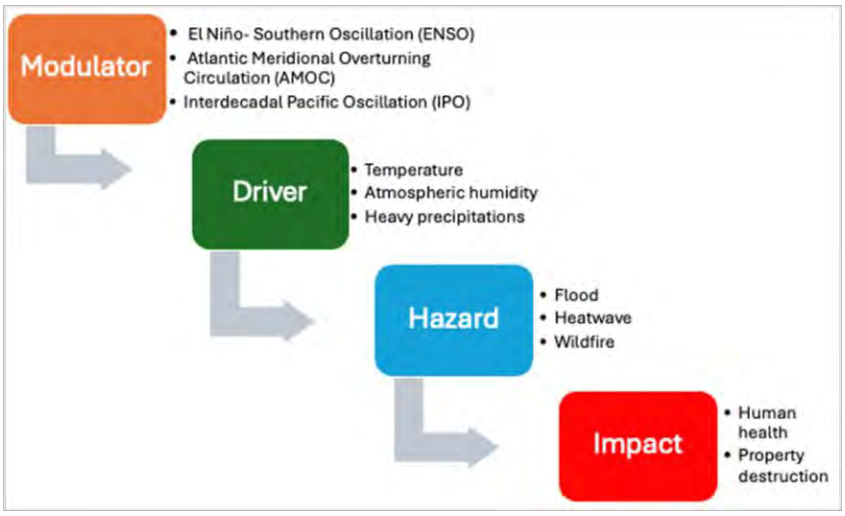


Typology of compound events - This classification of compound events delineates them into various types, with three that we are focusing on in this study:

- *Temporally compounding events* entail sequences of hazards resulting in impacts over time
- *Multivariate events* involve multiple factors or hazards converging to cause an impact
- *Spatially compounding events* happen when hazards coincide in space, leading to an impact

Each compound event type's underlying rationale, relevant atmospheric or climatic processes and their interactions are further illustrated with examples below:

Figure 1.2
KEY ELEMENTS FOR 3 TYPES OF COMPOUND EVENTS WITH EXAMPLES

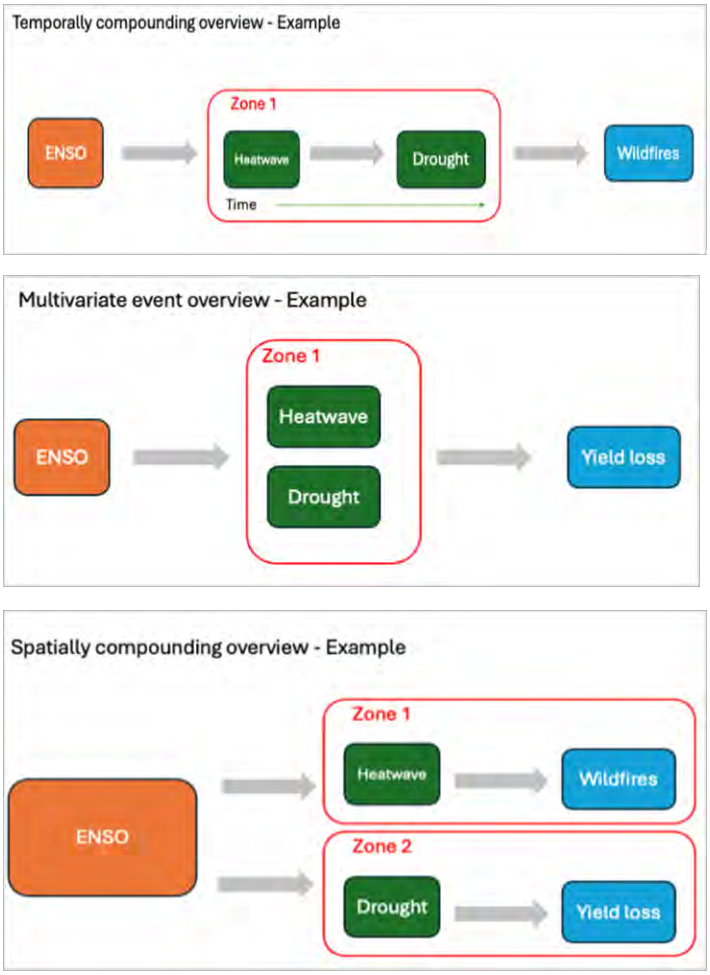


We acknowledged that there are other types of compound events apart from the three that are explored in this study, however, the three categories used cover most types. Compound event types are also based on subjective judgments, hence not all events neatly fit into a single type of compound event and would require flexible boundaries. For example, in coastal flooding events, large areas of low pressure cause flooding and heavy rain (multivariate event), but saturated soil (precondition) aggravates the flood damage as seen in the Netherlands in January 2012.

Bottom-up approach - Focusing on how different factors combine to create risks for society or the environment shows how crucial it is to first understand these risks before figuring out which factors are involved. This suggests using bottom-up approaches, which typically begin with a specific system or event (like a disaster), followed by looking at all the different factors that contribute to it. This includes figuring out which specific factors have the biggest impact.

Another benefit of bottom-up approaches lies in their capability to examine the impacts of hazards and the climate drivers of those hazards independently. This approach can prove to be effective in simultaneously

investigating multiple hazards and their underlying mechanisms. Given the anticipation that anthropogenic climate change will likely change the distributions of nearly all climate variables and some of their interdependencies, it is foreseeable that trends in the occurrence of compound events will emerge over decades to multi-decadal periods. Nonetheless, attributing changes in compound events to human-induced climate change poses challenges due to the limited sample size and low signal-to-noise ratio.

## 1.2 OBJECTIVES AND KEY QUESTIONS

Compound weather events research is a significant and rapidly growing field (Bevacqua, E (2023) , van den Hurk, B. J. J. M. (2023)), which involves collaboration across disciplines such as climate science, climate impacts, engineering, statistics and catastrophe modeling. The objective of this research is to enhance our understanding of risk and implications from compound events, including the probability and danger posed by such events. This improved understanding will also allow us to anticipate and make assumptions about projections in a future climate influenced by human activity.

Our proposed methodology focuses on climatic hazards like heatwaves and droughts with the goal to establish a causal relationship between compound climatic hazards and their impacts in terms of wildfire burned areas and crop yield. We aim to address three key questions:

1. Frequency: By how much does the probability of a hazard increase when two climatic drivers compound?
2. Severity: Are hazards triggered by compound events more destructive? If so, by how much?
3. Trend: How are compound events supposed to evolve in a warmer climate?

In the following, we attempted to answer these questions on specific use cases relying on recent literature and methodology, global data for meteorological variables and public data for hazards, as described in the section methodology.

## 1.3 SCOPE OF THE STUDY

This study focuses on three types of compound events. Temporally compounding events, that we call type 1; multivariate events, that we call type 2 and spatially compounding event, that we call type 3.

### *Temporally compounding events (i.e. type 1)*

Temporally compounding events (type 1) refer to a succession of hazards that affect a given geographical region (Zscheischler, J., 2020). In this part of the study, we look at positive temperature anomaly and drought hazards and explore how they affect the risk of wildfire in California. As discussed in the introduction, this work has been designed with a bottom-up approach, assuming the succession of positive temperature anomaly and drought at a one month lag at the same locations are at play for dangerous wildfire (Figure 1.3).

Figure 1.3
TEMPORALLY COMPOUNDING (TYPE 1) EVENT OVERVIEW

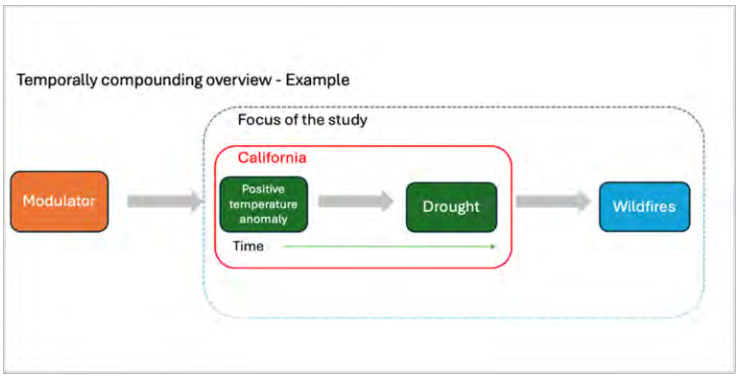


*Multivariate events (i.e. type 2)*

Multivariate events refer to the co-occurrence of multiple climate drivers and/or hazards in the same geographical region causing an impact (Zscheischler, J., 2020). In this research, the effect on the yield of the co-occurrence of drought and positive temperature anomaly during the flowering period of wheat is studied (Figure 1.4).

Figure 1.4
MULTIVARIATE EVENT OVERVIEW

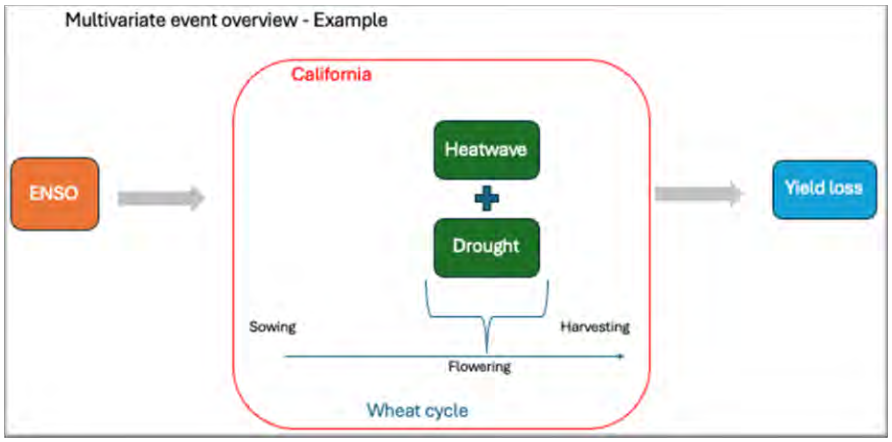


*Spatially compounding events (i.e. type 3)*

Spatially compounding events (type 3) occur when multiple connected locations are affected by the same hazard within a limited time window. In this part of this research, we focus on the role played by El Niño–Southern Oscillation (ENSO) and Atlantic Multidecadal Oscillation (AMO), two modulators of sea surface temperature in the Pacific and Atlantic oceans known to have teleconnections with the whole climatic system, and especially with tropical cyclone activity:

- El Niño–Southern Oscillation (ENSO), a climate phenomenon that exhibits irregular quasi-periodic variation in winds and sea surface temperatures over the tropical Pacific Ocean, affects the climate of much of the tropics and subtropics and has links (teleconnections) to higher latitude regions of the world. The warm phase of the sea surface temperature is known as El Niño and the cool phase as La Niña (Figure 1.5, WMO 2014);

- Atlantic Multidecadal Oscillation (AMO), also known as Atlantic Multidecadal Variability, is the theorized variability of the sea surface temperature (SST) of the North Atlantic Ocean on the timescale of several decades.

**Figure 1.5**
SEA SURFACE TEMPERATURE ANOMALIES DURING ENSO

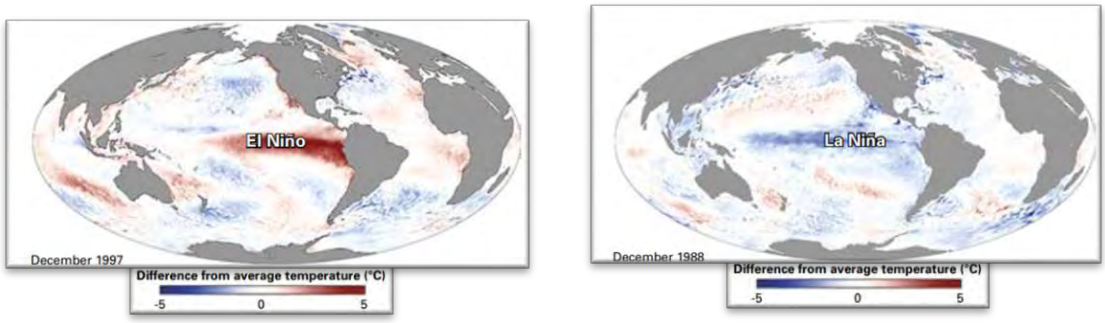


Credit: WMO, El Niño/Southern Oscillation (WMO-No. 1145). 2014

On the left panel, we observe an El Niño pattern with a positive temperature anomaly (red color) in the eastern south pacific. The right panel depicts a La Niña pattern with a negative temperature anomaly in the central south pacific.

These climate modulators are known to affect the tropical cyclone activity in different basins of the world. Our aim is to better understand the co-variability of tropical cyclone activity over all the tropical cyclone basins (Figure G in the Appendix) with ENSO and AMO changes.

**Figure 1.6**
SPATIALLY COMPOUNDING EVENT OVERVIEW

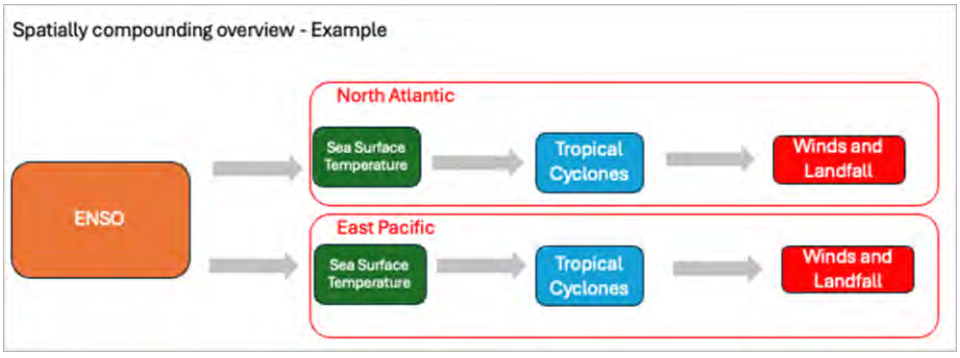


The following sections of this report detail the research results each type of the above mentioned compound events.

# Section 2: Temporally Compounding Events (Type 1)

In this section, we study the temporally compounding events (i.e., type 1) by understanding how compounding hazards (positive temperature anomaly and droughts) can impact wildfires risk.

## 2.1 HOW MUCH DOES THE PROBABILITY OF A WILDFIRE INCREASE WHEN TWO CLIMATIC HAZARDS COMPOUND?

The compound event of two climatic drivers, positive temperature anomaly and drought, is studied to compare the probability of having a wildfire, the hazard, given a dry condition, a hot condition and both compounded conditions. These three quantities are written as:

$$\text{Hot condition: } P(WF|H) \qquad \text{Dry condition: } P(WF|D) \qquad \text{Componded condition: } P(WF|D \cap H)$$

Where:

- "WF" denotes a wildfire
- "H" denotes a positive temperature anomaly one month before the wildfire
- "D" denotes a drought the month of the wildfire
- "|" is the symbol of conditioned probabilities, and is read as 'given'
- "∩" is the symbol for an intersection of events.

As we can only measure the probability of co-occurrence of these events, namely:

$$P(WF \cap H \ \cap D)$$

we, thus, use the Bayesian relation to deduce the conditioned probability from our measured ones:

$$P\left(WF_{|H\cap \mathrm{D}}\right) = \frac{P(WF \cap H \ \cap D)}{P(H \ \cap D)}$$

as similarly:

$$P\left(WF_{|H}\right) = \frac{P(WF \cap H\ )}{P(H\ )} \qquad and \qquad P\left(WF_{|D}\right) = \frac{P(WF \cap D\ )}{P(D)}$$

Note the probability of having a wildfire given a meteorological condition is mainly determined by the presence of a forest and a forest exposed to a wildfire risk. Nevertheless, such data are not straightforward to access nor easy to compute as forest presence doesn't mean a wildfire is likely. Hence, this study only considers locations where fire has been recorded and analyzes the climatic drivers on these locations from the observed period.

Figure 2.1
LOCATIONS OF WILDFIRES IN CALIFORNIA FROM 1984 TO 2020

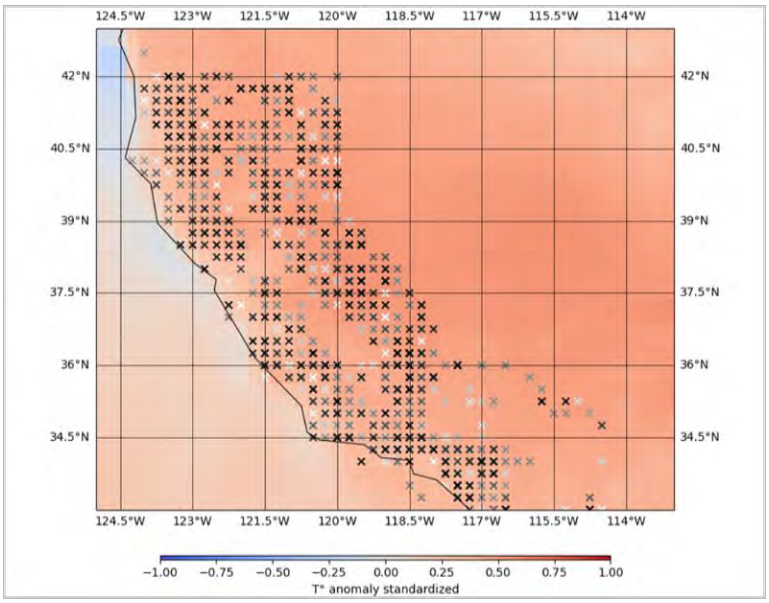


Note: The wildfires are represented by crosses. The most recent wildfires are in white, the oldest in black. More about the wildfire database and the standardized temperature anomaly in the Appendix.

To calculate each term of the equation, we need to count how many times each event happens and divide it by the number of observed points we have. For instance, to calculate $P(WF \cap H \cap D)$, we need to count the number of wildfires for a given positive temperature anomaly and drought and divide it by the total number of points. Similarly, to calculate $P(H \cap D)$, we count the number of points for a given positive temperature anomaly and drought condition divided by the total number of points.

Figure 2.2
JOINT PLOTS OF SPI-6-MONTH AND STANDARDIZED TEMPERATURE ANOMALY

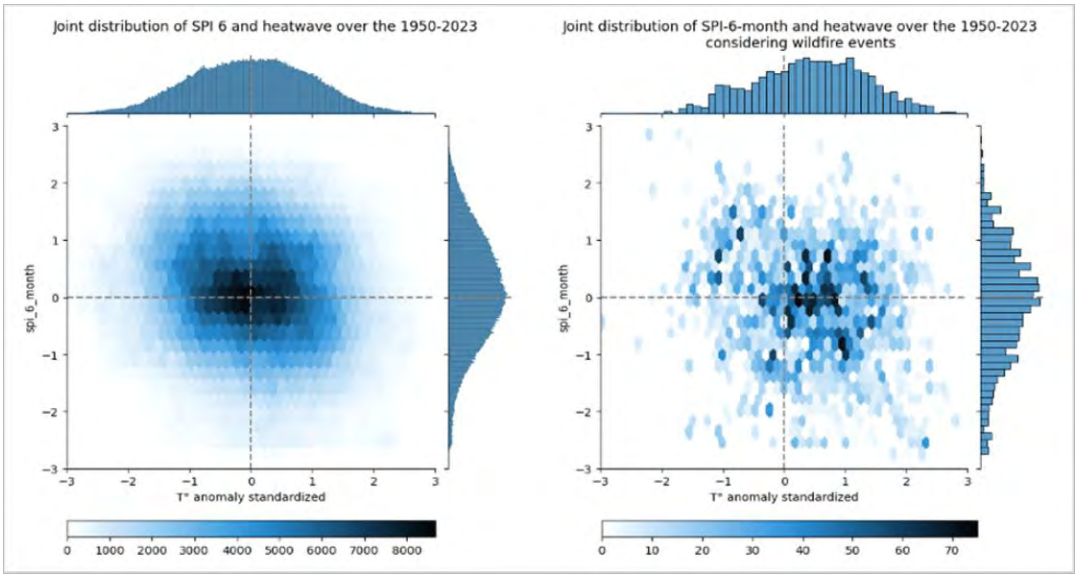


Note: The figure above displays the number of events that occurred for a given temperature anomaly (x-axis) and drought index (y-axis): (Left panel) shows the occurrence of combined condition for all exposed locations (i.e., where

there is a forest); (right panel) shows the occurrence of combined condition considering wildfire events only. More about SPI and standardized temperature anomaly in the Appendix.

As Figure 2.2 shows, while all the combinations of temperature anomaly and drought index are possible, some happen more frequently and are presented through hexagonal bins (the darker the color, the higher the occurrence of the event). We observed there to be mostly neutral conditions, i.e., temperature anomaly and drought index both equal to 0, whereas patterns change when we only pick conditions when wildfires are triggered (right panel).

**Figure 2.3**

PROBABILITY OF HAVING WILDFIRE GIVEN DROUGHT (D), HEAT (H) OR DROUGHT AND HEAT (D∩H)

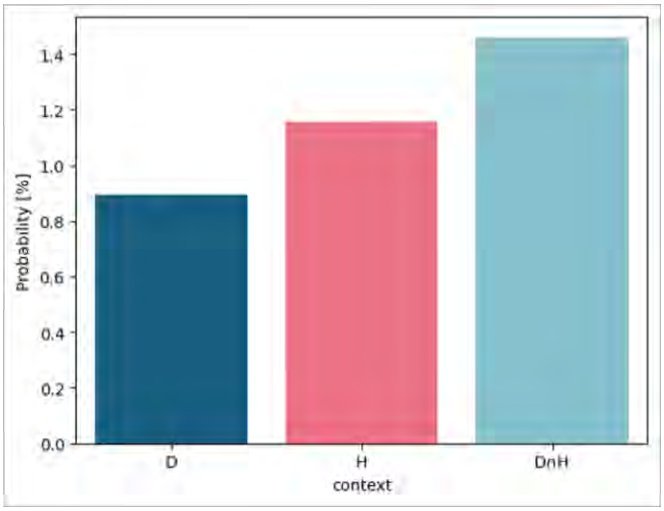


Note: Probability of having a wildfire given drought (D) or heat (H) or drought and heat (DH) in which: D = (SPI-6-month < -1); H = ( standardized T° anomaly month m-1 >1); and D∩H = ( SPI-6-month <-1 and standardized T° anomaly month m-1> 1).

When comparing probabilities of having a wildfire under single or compound conditions, as shown in Figure 2.3 above, it appears that wildfires are more likely to appear during compound events compared to single events, with a 62% increase comparing single event D to compound events, D∩H, and a 26% increase by comparing a single event to compound events. However, it is important to note that wildfires are still a rare event with the probability of happening around 1% when we take into consideration the whole year.

## 2.2 DO COMPOUND EVENTS EXTEND THE FIRE SEASON?

To assess how compound events can affect wildfire intensity, we looked at how compound events would extend the fire season. By looking at the probability of having wildfire by season under different single or compound event contexts, we could investigate whether compound events increase the risks of having wildfires inside and outside of fire season extending the fire season. Figure 2.4 below shows the fire season can be defined as June to October given most wildfires happen during this time window.

Figure 2.4
OCCURRENCE OF WILDFIRE DURING YEAR IN CALIFORNIA

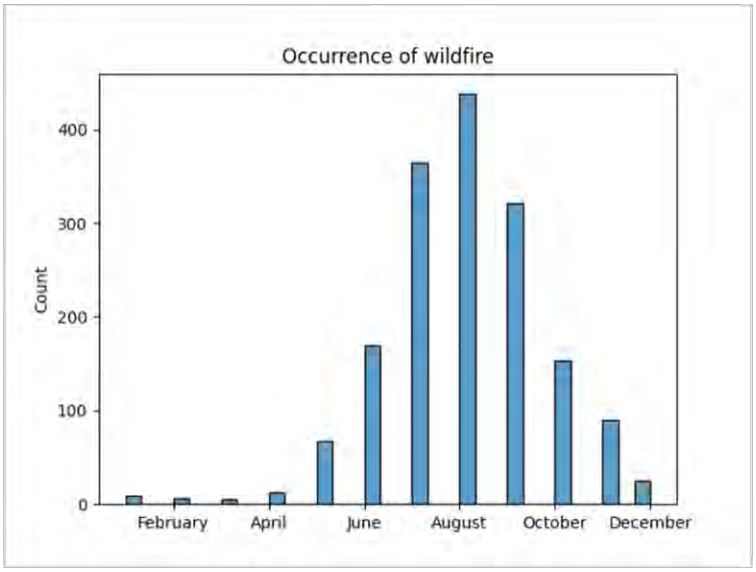


Figure 2.5
PROBABILITY OF HAVING WILDFIRE DURING WILDFIRE SEASON AND DURING WHOLE YEAR GIVEN DIFFERENT SINGLE EVENT (D OR H) AND COMPOUND EVENT (D∩H) CONTEXTS

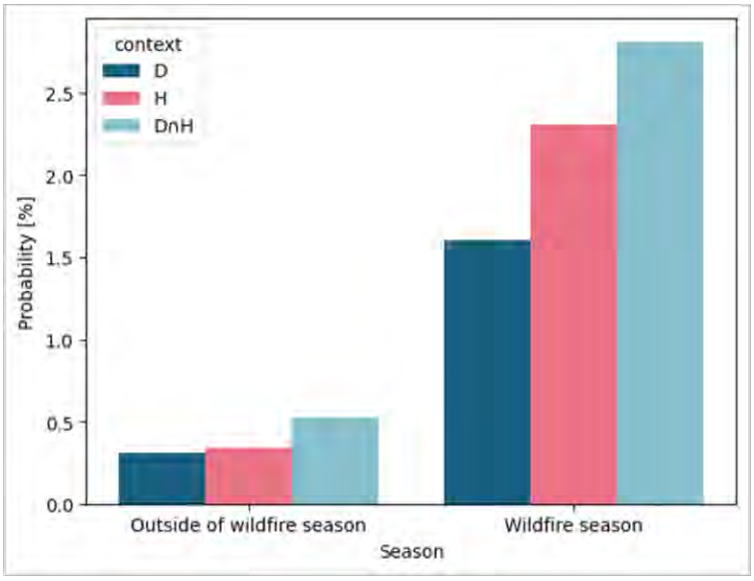


Note: Probability computed based on wildfires from 1984 to present. Wildfire season ranges from June to October based on the above figure.

When comparing the probability of having a wildfire inside the fire season to the probability of having a wildfire outside, Figure 2.5 above demonstrates an increase in wildfire risk both during and after the wildfire season. The risk increase is higher during the wildfire season than outside for compound events (75% and 22% increase from drought and heat event compared to compound events during the wildfire season; 71% and 56% for drought and heat compared to compound events outside the wildfire season).

We observe the same order of risk depending on the context during and after the wildfire season, with compound events being riskier than high temperature anomaly or drought alone. Differences between probabilities were statistically different at 5% error risk based on chi square test.

# Section 3: Multivariate Compounding Events (Type 2)

In this section, we study the multivariate compounding events (i.e., type 2) by understanding how compounding positive temperature anomaly and droughts can impact yield loss of winter wheat, with focus on the indicator during the flowering period of which the plant is the most susceptible to yield loss. Based on literature review, we have identified winter wheat flowering period in California to be between April to May, which is the time months in which we tailor the indicators for its specific flowering period.

## 3.1 HOW MUCH DOES THE PROBABILITY OF YIELD LOSS INCREASE WHEN TWO CLIMATIC HAZARDS COMPOUND?

Contrary to the wildfire analysis, a lag between drought and positive temperature anomaly was not considered, but instead we only focused on the co-occurrence of drought and positive temperature anomaly during the flowering period. Data for drought and temperature anomaly were also adapted accordingly:

- **Drought index:** we use SPI-2-month in May to accurately represent the drought for the months of April and May. SPI-2-month computation can be derived from the 2.1.2 SPI formula described, using a two-month rolling window;
- **Temperature index**: we compute the average temperature for the period April-May, then compute the standardized temperature anomaly on this period.

Regarding the yield data, we selected the 2005-2022-time window to limit the influence from technological improvement to agriculture (please refer to 'Data and methodology note' section for more details). We then standardize the yield using the following formula:

$$Z(lat, lon, year) = \frac{Yield(lat, lon, year) - \overline{Yield}(lat, lon)}{\sigma_{yield}(lat, lon)}$$

Figure 3.1

YIELD EVOLUTION OF SPRING WHEAT FROM 2005 TO 2022 (LEFT) AND DETRENDED YIELD (RIGHT)

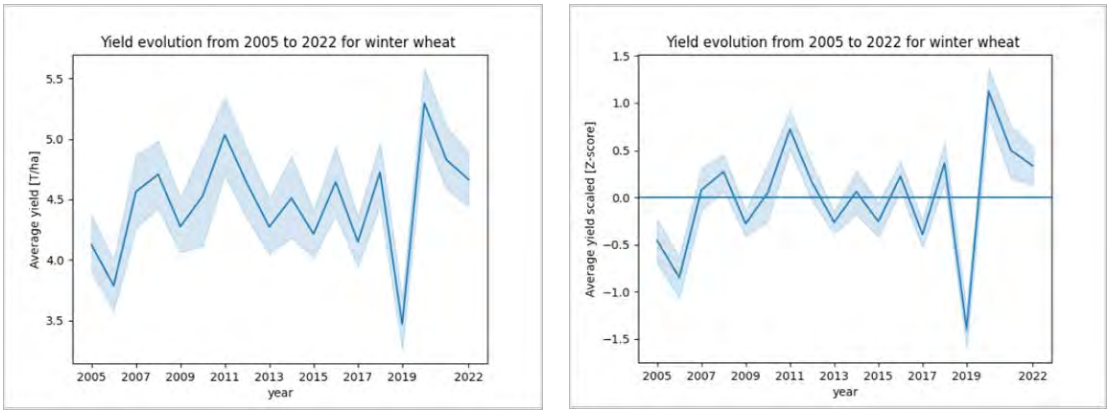


To study the effect of compound events on yield loss, we will be dealing with the standardized yield as seen on the right of Figure 3.1, with yield loss described as having a standardized yield below zero.

Figure 3.2

WINTER WHEAT YIELD (BY VARIOUS EXTENT) AGAINST JOINT DISTRIBUTION OF SPI-2 MONTHS (Y-AXIS) AND TEMPERATURE ANOMALY (X-AXIS)

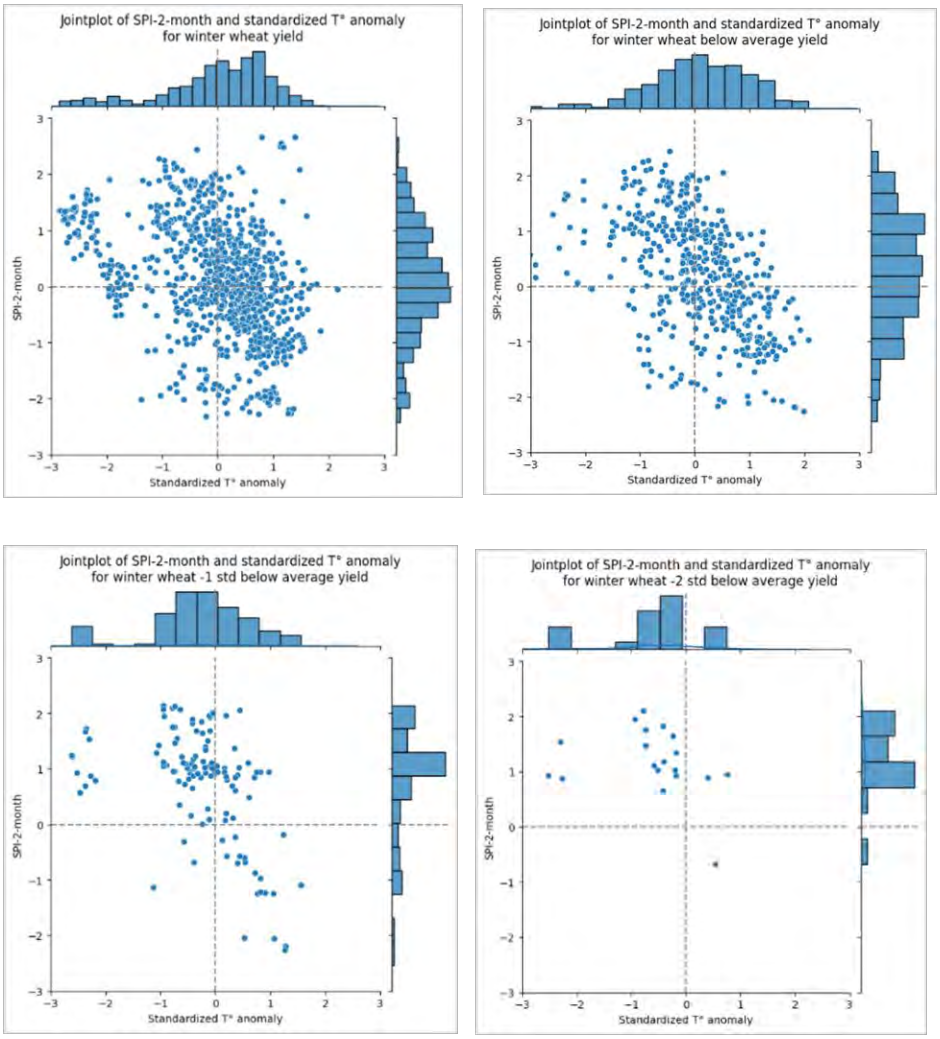


From Figure 3.2, the top-left chart displays the full data on winter wheat yield, in which we observe most flowering periods happen in normal conditions as the density is higher around the center (close to 0). Moving from the top right to bottom left and bottom right charts, as we increase the yield loss data value from less than the average ( <0 std ) to a large departure from the average (-2 std, or bottom ~3.5%), emphasizes the evolution of the joint distribution when the yield loss increases.

When considering one standard deviation from the mean, it appears that yield loss is trending towards high positive temperature anomaly and drought (bottom right quadrant) as the shift in temperature anomaly and spi-2-months distributions suggest.

Figure 3.3
PROBABILITY OF YIELD LOSS GIVEN DIFFERENT CONTEXTS

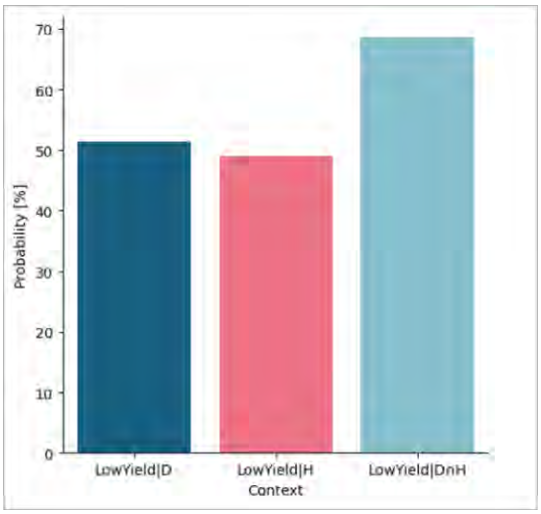


Note: Figure 3.3 displays the probability of yield loss given different contexts, where: H = standardized temperature anomaly > 1; D = spi-2-months <-1; and D∩H = spi-2-months <-1 and standardized temperature anomaly > 1.

When looking at the low yield probability results under single or compound event conditions (as shown in Figure 3.3), there is indeed a strong link between low yield and compound events, with 70% risk of having a yield below average when dealing with a compound event, contrary to single events that do not impact crop yield as greatly.

However, keep in mind that when comparing the statistical significance of our finding using the chi square test, the probability differences were not significant at a 5% error risk. It is also important to note this study focused on compound events of drought and positive temperature anomaly and overlooked other sources of yield loss such as frost, excess of water, pests, etc.

To illustrate, in Figure 3.2 we observe the largest yield loss variance from the mean happens with cold and wet weather during the flowering period. This finding supports the idea that heat and drought are not the sole drivers of yield loss, while acknowledging the other drivers mentioned above are outside the scope of this study.

## 3.2 ARE YIELD LOSSES TRIGGERED BY COMPOUND EVENTS MORE SEVERE?

To assess the intensity of yield loss under different contexts, we plotted the yield distribution associated with the events.

We observe slight differences in the median yield regardless of the context. Compound events lead to a median yield 7% below the average, whereas single events lead to slightly higher yield than the average (2% and 3% higher than average, respectively, for drought and high temperature anomaly contexts). When comparing maximum positive yield differences to the mean, compound events also demonstrate lower probable maximum yield when compared to single events.

Figure 3.4
DISTRIBUTION OF YIELD DIFFERENCE TO MEAN GIVEN DIFFERENT CONTEXTS

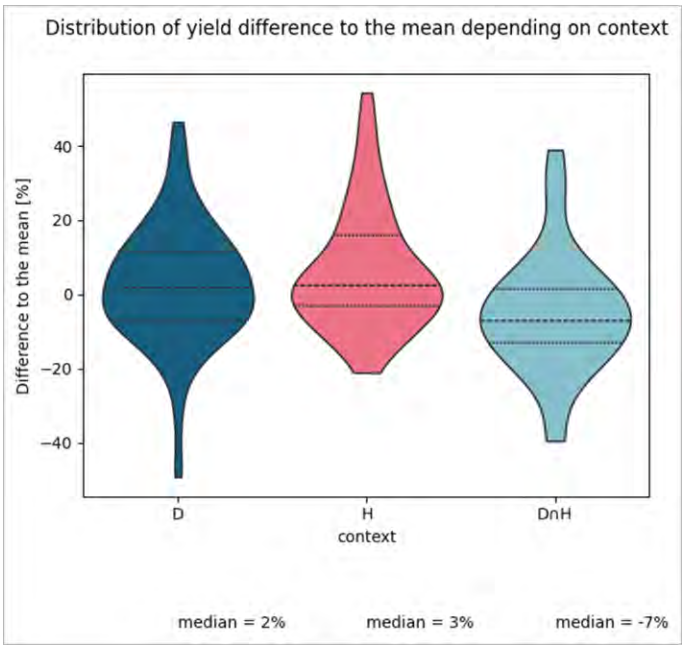


However, observations other than the median and maximum yield difference to the mean should not be overlooked. For instance, a single drought event happens to show the most catastrophic yield with its maximum negative yield (-50%) exceeding the one of compound events (-40%). As a result, this study on compound events on winter wheat concludes a moderate correlation between yield loss and compound events.

As a side note, despite cold and wet weather context, which was observed previously as a strong compound event driver for yield loss and not covered in this study, it can be expected that such compound event context will be even more destructive, especially exacerbated by the little to no management practices to mitigate such an event.

## Section 4: Spatially Compounding Events (Type 3)

In this section, the correlation between the climate modulators, El Niño–Southern Oscillation (ENSO) and Atlantic Multidecadal Oscillation (AMO), and the tropical cyclone intensity, frequency and spatial distribution is analyzed. This type of analysis has been performed to study the correlation between climate modulators and various types of drivers or hazards on a local or global scale (Tiwari et al., 2022; Lloyds emerging risk report, 2016).

We start by looking at the *time series* of Niño 3.4 and the tropical cyclone activity (frequency and intensity) over each tropical cyclone basin (see Figure G in the methodology section of the Appendix). The analysis is also reproduced with the AMO index. Next, we quantify the *correlation* between Niño 3.4 and the tropical cyclone activity (frequency and geographical distribution) over each basin. Similarly, the analysis is reproduced with the AMO and the tropical cyclone frequency. Finally, a *correlation matrix* is computed to highlight the links between the two climate modulators (Niño 3.4 and AMO) and the tropical cyclone frequency and intensity.

The climate modulators (Niño 3.4 and AMO) are computed every year as the average over each hemisphere's tropical cyclone season:

- Southern hemisphere: October (previous year) to April
- Northern hemisphere: June to November

The tropical cyclone metrics are computed annually over:

- Southern hemisphere: October (previous year) to September
- Northern hemisphere: January to December

The intensity of tropical cyclone season is computed as the average Accumulated Cyclone Energy (ACE) over storms reaching a tropical storm status (wind speed >= 34 knots).

The frequency of the tropical cyclone season is computed as the total number of tropical cyclones and the very intense tropical cyclones (category 3+ on the Saffir-Simpson hurricane wind scale).

### 4.1 TIME SERIES ANALYSIS OF TROPICAL CYCLONE COUNTS AND ACCUMULATED CYCLONE ENERGY RELEASED AGAINST NINO 3.4 AND AMO INDICES

*Nino 3.4 index*

The Niño 3.4 index provided by the NOAA CPC (see the Data section in the Appendix) averaged over the tropical cyclone seasons of both hemispheres is considered an El Niño year when the index (sea surface temperature anomaly) is above 0.5°C, and is considered a La Niña year when the index is below -0.5°C.

In the Southern Hemisphere basins (South Indian and South Pacific), the years considered:

- El Niño years are: 1982/83, 1986/87, 1991/92, 1994/95, 1997/98, 2002/03, 2009/10, 2014/15, 2015/16, 2018/19, 2023/24
- La Niña years are: 1983/84, 1984/85, 1985/86, 1988/89, 1995/96, 1998/99, 1999/00, 2000/01, 2005/06, 2007/08, 2008/09, 2010/11, 2011/12, 2017/18, 2020/21, 2021/22, 2022/23

In the Northern Hemisphere basins (East Pacific, North Atlantic, North Indian, West Pacific), the years considered:

- El Niño years are: 1982, 1987, 1991, 1997, 2002, 2004, 2009, 2015, 2023
- La Niña years are: 1983, 1984, 1985, 1988, 1989, 1995, 1998, 1999, 2000, 2007, 2010, 2011, 2020, 2022

The time series of Niño 3.4 and the tropical cyclone frequency over each basin is displayed in Figure 4.1 below. The total tropical cyclone count (reaching at least a category 1 intensity) is displayed in light green and the very intense tropical cyclone count (reaching at least a category 3 intensity) is displayed in dark green. The Niño 3.4 index values can be read on the y-axis (on the left), and the tropical cyclone counts on the secondary y-axis (on the right).

ENSO follows an irregular cycle, with each episode of El Niño or La Niña lasting from 9 to 12 months, though some events may persist longer. El Niño and La Niña occurrences are irregular but typically happen every two to seven years.

The West Pacific basin has the highest numbers of tropical cyclones each year, with an average of 16 events per year since 1982, followed by the East Pacific with nine events, the South Indian with eight events, the North Atlantic with six events, the South Pacific with four events, and the North Indian with two events.

Over the Pacific Ocean basins (EP, WP and SP), the highest activity with an El Niño year (in red) and the lowest tropical cyclone activity coincides with La Niña years (in blue). In the North Atlantic, the opposite is true, with the highest (lowest) activity coinciding with La Niña (El Niño) years. In the North and South Indian basins, no clear relationship can be determined by analyzing this time series.

Figure 4.1
TIME SERIES OF NIÑO 3.4 INDEX AND CYCLONE COUNTS FOR EACH BASIN

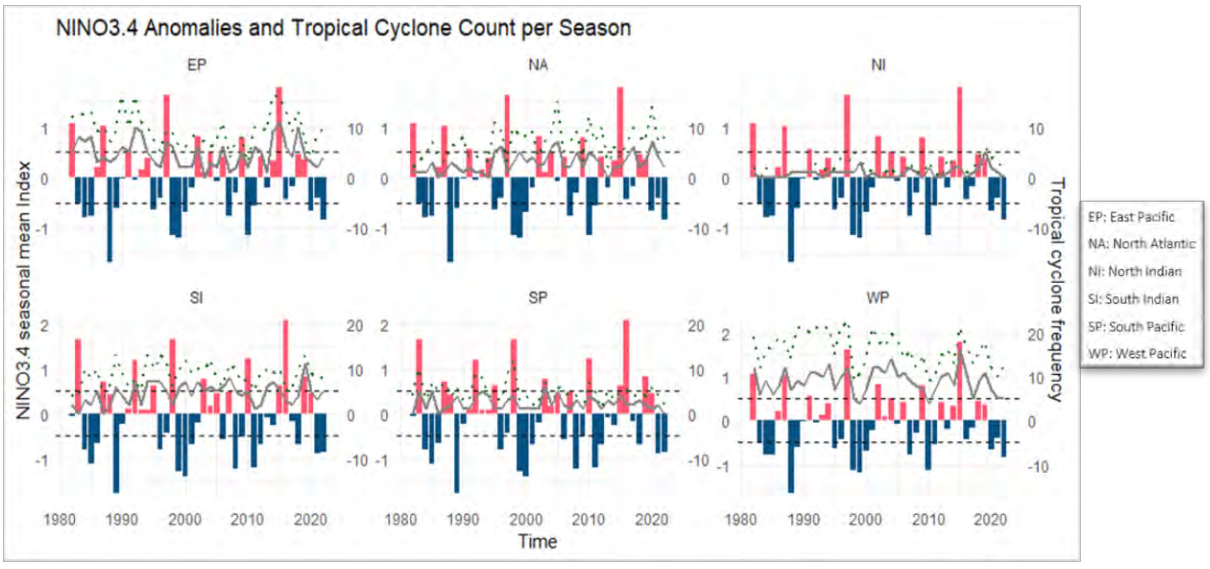


Note: The figure above displays the El Niño 3.4 index timeseries on the left y-axis, and the category 1 to 5 cyclone counts (dotted green) and the category 3 to 5 cyclone counts (dark green) on the right y-axis for each basin.

Looking into the annual average energy released by tropical cyclones (ACE) per basin (Figure 4.2 below in pink), the West Pacific also displays the strongest intensity, with an average cyclone ACE of 11.25 $10^4$knot$^2$, followed by the North Atlantic with an average cyclone ACE of 8.6 $10^4$knot$^2$, the South Indian with 8.1 $10^4$knot$^2$, the East Pacific with 7.8 $10^4$knot$^2$, the South Pacific with 7.2 $10^4$knot$^2$ and, finally, the North

Indian with 4.2 $10^4$knot$^2$. It appears that the tropical cyclone basins with the largest (smallest) frequency of events also generate the most (least) powerful events on average.

The West Pacific and South Pacific basins show the strongest (weakest) ACE during El Niño (La Niña) years. The opposite is true over the North Atlantic basin. We can conclude that the frequency, intensity and ACE metrics all follow the same relationship with the ENSO index.

**Figure 4.2**
TIME SERIES OF NIÑO 3.4 INDEX AND AVERAGE ACE FOR EACH BASIN

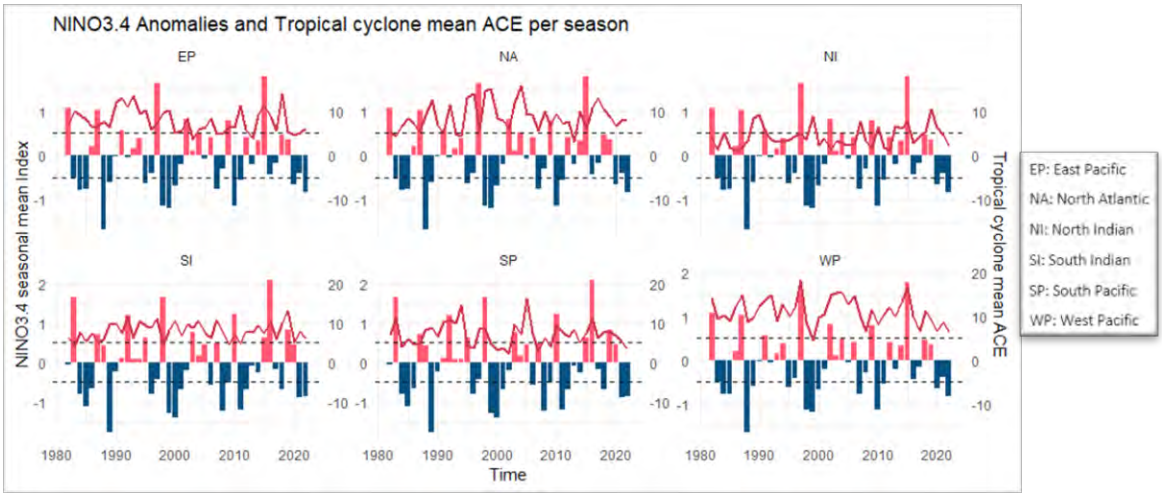


Note: The figure above displays the El Niño 3.4 index timeseries on the left y-axis and the average ACE on the right y-axis for each basin.

### *AMO index*

The AMO index provided by the NOAA PSL (see the Data section in the Appendix) is averaged over the tropical cyclone seasons of both hemispheres from 1980 to 2023 (Figure 4.3). The positive phase of the index, illustrated in red (right y-axis), started in the mid-1990s, and the negative phase of the index occurred before that. Analyzing the AMO index starting as early as 1950 would capture a complete cycle of both positive and negative AMO phases and, therefore, enhance the robustness of the conclusions. However, since the tropical cyclone monitoring system was less reliable before 1980, prior to the use of satellite technology, we chose to start our analysis in 1980.

Looking at the total number of tropical cyclones (light green), **the Pacific Ocean (EP, WP, SP)** seems to follow a **negative trend** with a higher number of tropical cyclones before the mid-1990s, except around 2014-2015 in the East Pacific. The **North Atlantic** seems to follow a **positive trend** overall, which is consistent with the switch of the AMO index from a negative to a positive phase. The current positive phase corresponds to warmer sea surface temperatures in the North Atlantic that provides moisture in the atmosphere that fuels tropical cyclone developments. The trends are not clear for the high intensity storms (dark green).

Figure 4.3
TIME SERIES OF AMO AND CYCLONE COUNTS FOR EACH BASIN

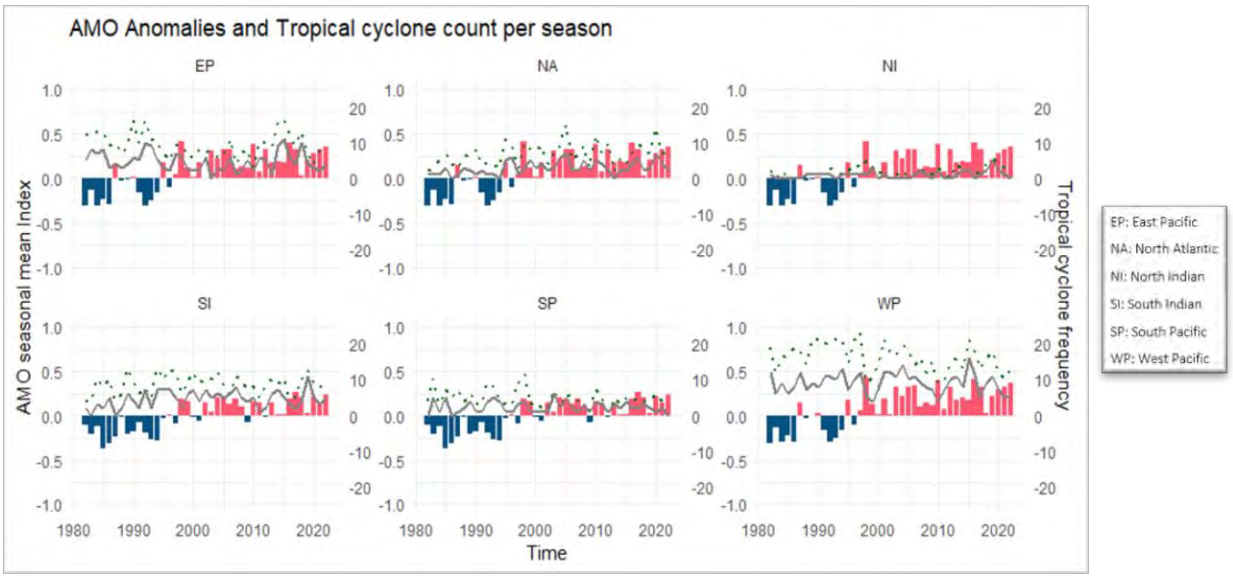


Note: The figure above displays the AMO index timeseries on the left y-axis, and the category 1 to 5 cyclone counts (dotted green) and the category 3 to 5 cyclone counts (dark green) on the right y-axis for each basin.

Looking into the annual average of the energy released by tropical cyclones (ACE) per basin (Figure 4.4 below in pink), the **Pacific Ocean basins (EP, WP, SP)** also appear to display a **negative trend**. Over the **North Atlantic basin**, the trend seems to be **positive,** which is coherent with the current warm phase of the AMO, which can provide more energy to sustain the development and intensification.

Figure 4.4
TIME SERIES OF AMO INDEX AND AVERAGE ACE FOR EACH BASIN.

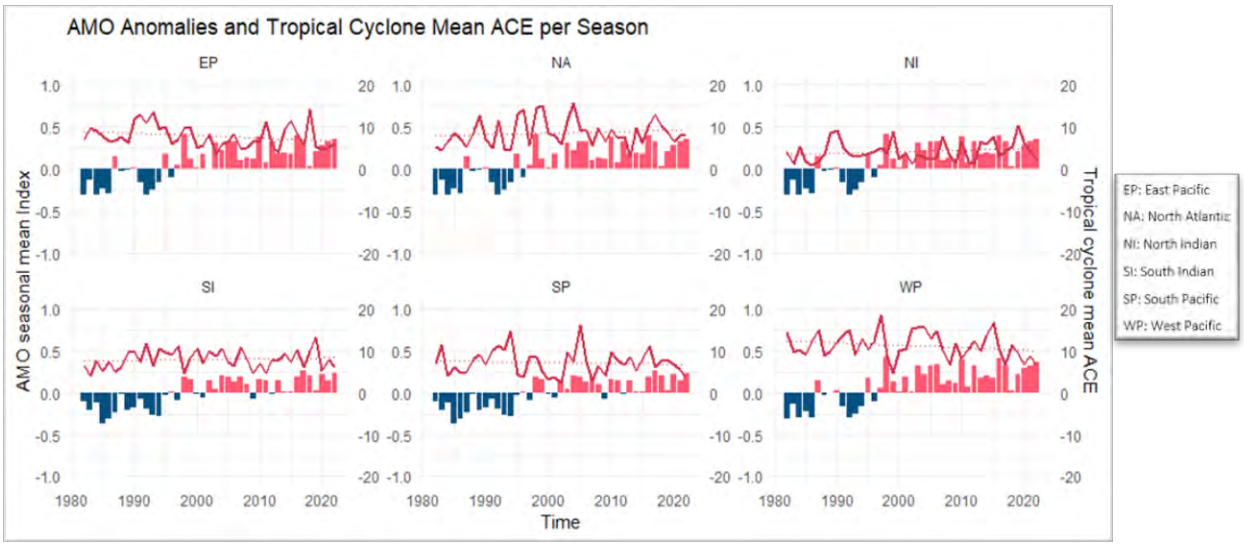


Note: The figure above displays on the left y-axis the AMO index timeseries and the average ACE on the right y-axis for each basin.

## 4.2 HOW DO THE NINO 3.4 INDEX AND AMO INDEX CORRELATE WITH TROPICAL CYCLONE ACTIVITY?

In the previous chapter, the tropical cyclone frequency, intensity and ACE metrics appear to follow similar behavior with respect to the ENSO and AMO modulators. In Figure 4.5 below, we explore the correlation between the tropical cyclone frequency metric (the number of tropical cyclone events of category 1 to 5) and intensity metric (the average tropical cyclone ACE). The two metrics are positively correlated, meaning that the years with the largest (smallest) number of tropical cyclones are also years with the most (least) intense events on average.

We, therefore, chose to only analyze the tropical cyclone frequency metric in this chapter (Figures 4.6 and 4.7). In addition, we explore the relationship between ENSO and the spatial distribution of the tropical cyclone activity (Figures 4.8 and 4.9).

Figure 4.5
CYCLONE COUNT ANOMALY AND AVERAGE ACE ANOMALY FOR EACH BASIN

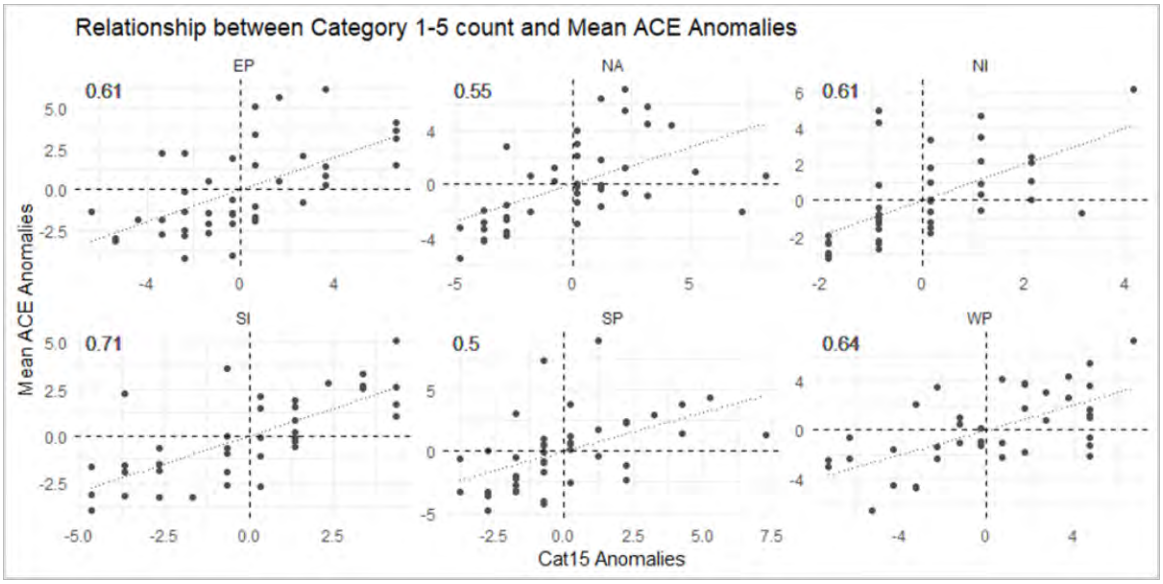


Note: The above scatter diagram displays the category 1 to 5 count anomaly (x-axis) and the average ACE anomaly (y-axis) for each basin (EP = East Pacific, NA = North Atlantic, NI = North Indian, SI = South Indian, SP = South Pacific, WP = West Pacific).

The correlation between Niño 3.4 and the anomaly of the tropical cyclone count over each basin is displayed in the scatter plot (Figure 4.6) below. The y-axis corresponds to the total tropical cyclone count anomaly (reaching at least a category 1 intensity, displayed in red) and the very intense tropical cyclone count anomaly (reaching at least a category 3 intensity, displayed in blue). The Niño 3.4 index values can be read on the x-axis. The statistical significance of the correlations is not analyzed here; however, it is addressed in the correlation matrix section in Figure 4.10.

The strongest positive correlation occurs in the West Pacific for both very intense and total number of tropical cyclones. The East Pacific and South Pacific also display positive correlations for the two types of cyclones. The North Atlantic shows a negative correlation with the highest tropical cyclone activity (displayed as the tropical cyclone count anomaly) occurring during La Niña years. The South Indian basin total tropical cyclone activity is negatively correlated to the Niño 3.4 index, but the correlation disappears

when looking into the very intense tropical cyclones. The North Indian basin does not show any correlation to the Niño 3.4 index.

**Figure 4.6**
NIÑO 3.4 INDEX AND ANOMALY OF CYCLONE COUNTS FOR EACH BASIN

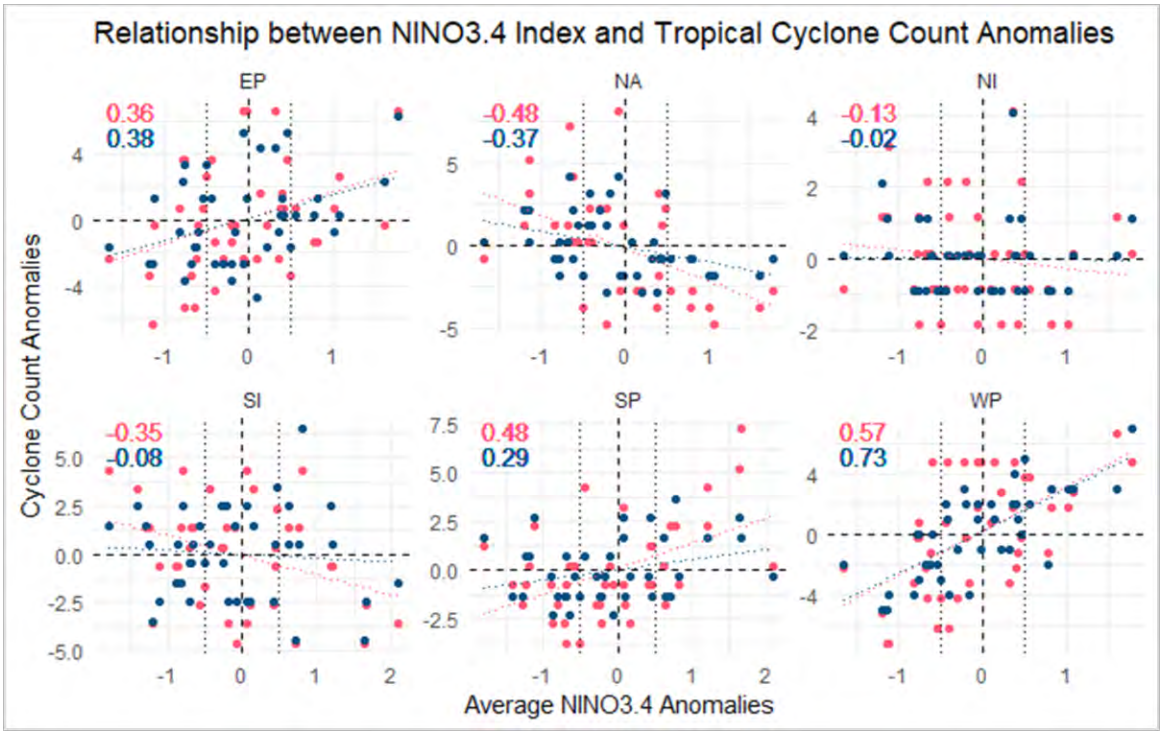


Note: The scatter diagram displays the Niño 3.4 index (x-axis) and the anomaly of the category 1 to 5 cyclone counts (red) and category 3 to 5 cyclone counts (blue) (y-axis) for each basin (EP = East Pacific, NA = North Atlantic, NI = North Indian, SI = South Indian, SP = South Pacific, WP = West Pacific).

The correlation between the AMO and the anomaly of the tropical cyclone count over each basin is displayed in the scatter plot (Figure 4.7) below. The y-axis corresponds to the total tropical cyclone count anomaly (in red) and the very intense tropical cyclone count anomaly (in blue). The statistical significance of the correlations is not analyzed here; however, it is addressed in the correlation matrix section in Figure 4.10.

The strongest positive correlation occurs in the North Atlantic for both very intense and total number of tropical cyclones. Warmer sea surface temperatures corresponding to the current positive phase of the AMO favors the development and intensification of tropical cyclones in the Atlantic.

The AMO index appears to have an influence on the Pacific Ocean. The total number of cyclones in the West Pacific, East Pacific and South Pacific basins are negatively correlated with the AMO. Recent studies have highlighted the influence of the positive phase of the AMO on the weakening of the Western North Pacific and South Pacific tropical cyclone activity (Sun et al., 2017; Zhang et al., 2018; Huang et al., 2023). The AMO positive phase has been linked to a warming over the subtropical North Pacific leading to changes in the atmospheric western tropical Pacific region. The positive AMO phase has also been associated with the strengthening of the Walker Circulation and, therefore, an increased vertical windshear (Huang et al., 2023; Levine et al., 2017). As a reminder, the Walker Circulation is an equatorial atmospheric circulation

with rising air over the western Pacific and sinking air over the eastern Pacific, which weakens during El Niño (warming in the central/eastern Pacific) and strengthens during La Niña (cooling in the eastern Pacific), driving the trade wind and weather pattern changes associated with ENSO.

**Figure 4.7**
AMO INDEX AND ANOMALY OF CYCLONE COUNTS FOR EACH BASIN

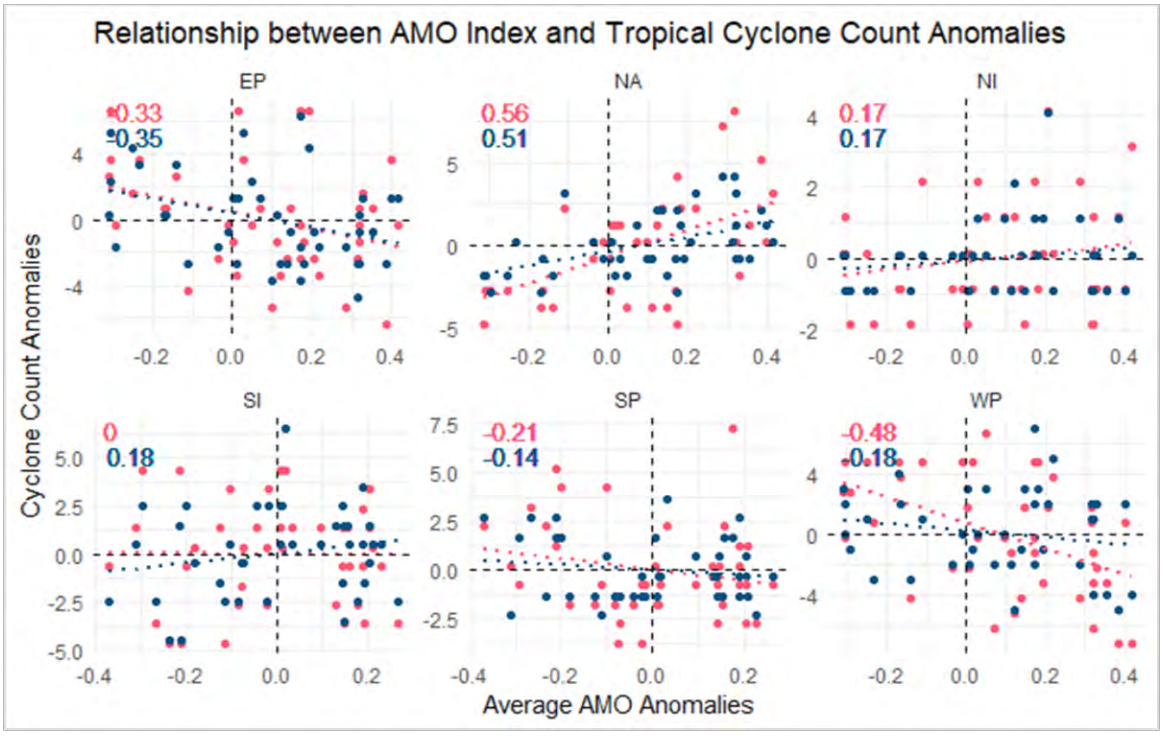


Note: The scatter diagram displays the AMO index (x-axis) and the anomaly of the category 1 to 5 cyclone counts (red) and category 3 to 5 cyclone counts (blue) (y-axis) for each basin (EP = East Pacific, NA = North Atlantic, NI = North Indian, SI = South Indian, SP = South Pacific, WP = West Pacific).

The correlation between Niño 3.4 and the anomaly of the average latitude of maximum winds per basin is displayed in the scatter plot (Figure 4.8) below. A positive (negative) anomaly in the average latitude of maximum winds means that the latitude is closer to the pole (equator) in the Northern Hemisphere and closer to the equator (pole) in the Southern Hemisphere.

In the Pacific Ocean, during El Niño (La Niña) events, the latitude of maximum winds tends to occur closer to the equator (poles) with negative (positive) anomalies in the West and East Pacific basins and a positive (negative) anomaly in the South Pacific. ENSO does not seem to influence the latitude of maximum winds over the North Atlantic, the North Indian or the South Indian basins. The average latitude of maximum winds is displaced by 2° to 4° of latitude, which is equal to 222 km to 444 km at the poles.

Figure 4.8
THE NIÑO 3.4 INDEX AND ANOMALY OF AVERAGE LATITUDE OF MAXIMUM WINDS FOR EACH BASIN

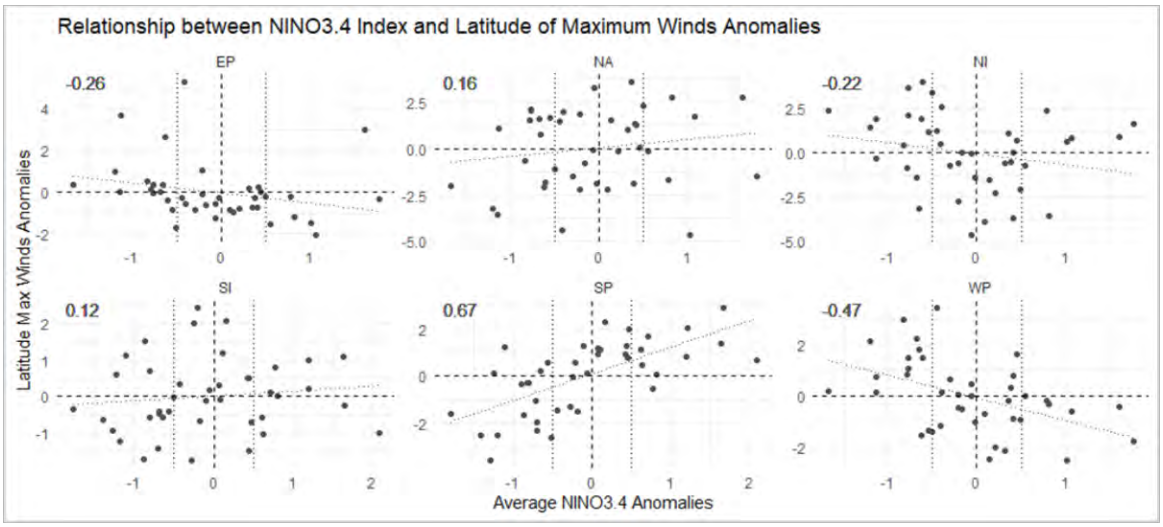


Note: The scatter diagram displays the Niño3.4 index (x-axis) and the anomaly of the average latitude of maximum winds (y-axis) for each basin (EP = East Pacific, NA = North Atlantic, NI = North Indian, SI = South Indian, SP = South Pacific, WP = West Pacific).

We then study the average tropical cyclone's location during El Niño and La Niña years as the total number of tracks within 2° x 2° grid boxes. For each basin, Figure 4.9 shows the El Niño average track count on the left, the average La Niña track count in the center, and the difference between El Niño and La Niña average track counts on the right.

Over the **West Pacific,** the tracks during El Niño appear to occur east of the Philippines and mainland China, close to Micronesia and Guam Island. During La Niña, tropical cyclones tend to be displaced towards the Western part of the basin, closer to Vietnam, the Chinese coastline and the Philippines. Over the **East Pacific**, the tracks are located towards the west side of the basin near Hawaii during El Niño, and shift towards the Mexican coastline during La Niña. In the **North Atlantic**, the track density is much larger during La Niña, which influences the results, showing a larger number of tracks close to the U.S., Mexican and Caribbean coastlines during La Niña years. The **North Indian** basin appears to have more events near the Northeast coast of India and Bangladesh during El Niño. The **South Pacific** basin does not have a clear shift in the track location but, during El Niño, it seems like the tropical cyclone activity occurs closer to Vanuatu and the South coast of Queensland than during La Niña. Finally, in the **South Indian** basin, there is a larger number of tropical cyclone tracks close to the Australian coastline and between the southern end of Madagascar and the Mozambique coastline during La Niña.

Figure 4.9

AVERAGE NUMBER OF TRACKS DURING EL NIÑO YEARS, LA NIÑA YEARS AND DIFFERENCES BETWEEN EL NIÑO AND LA NIÑA COUNTS

West Pacific

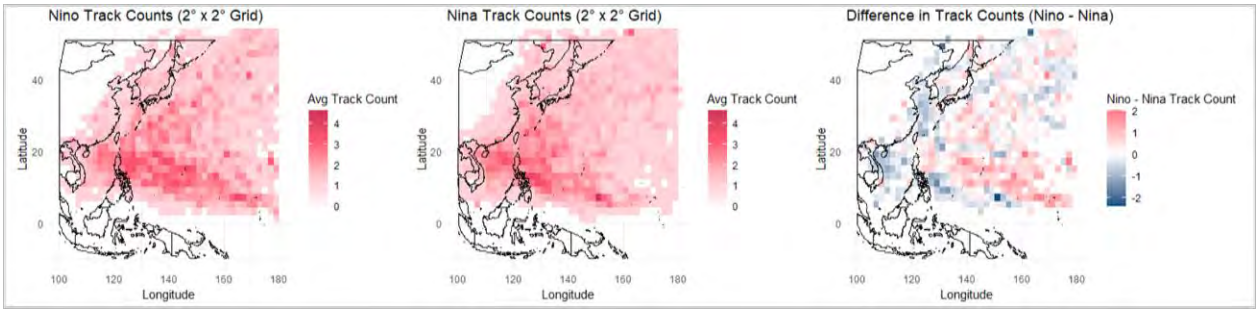


East Pacific

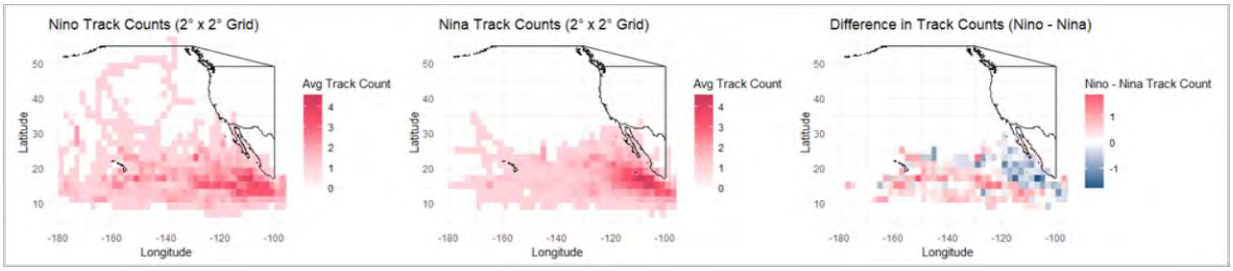


North Atlantic

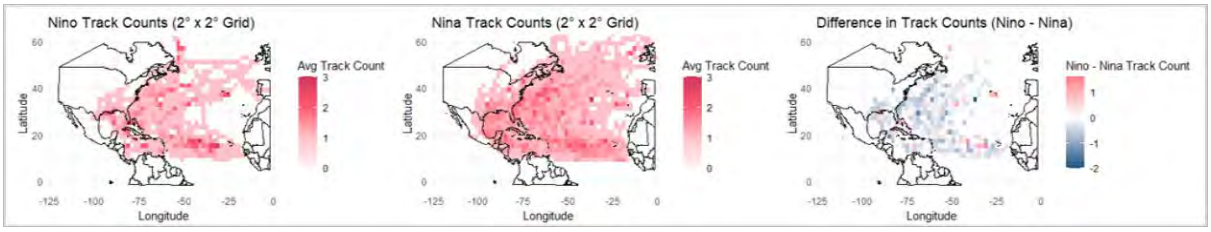


North Indian

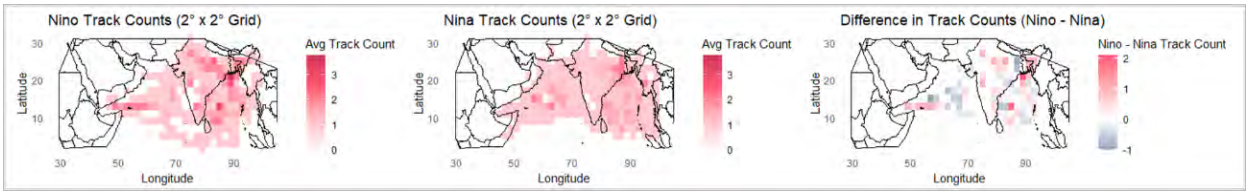

South Pacific

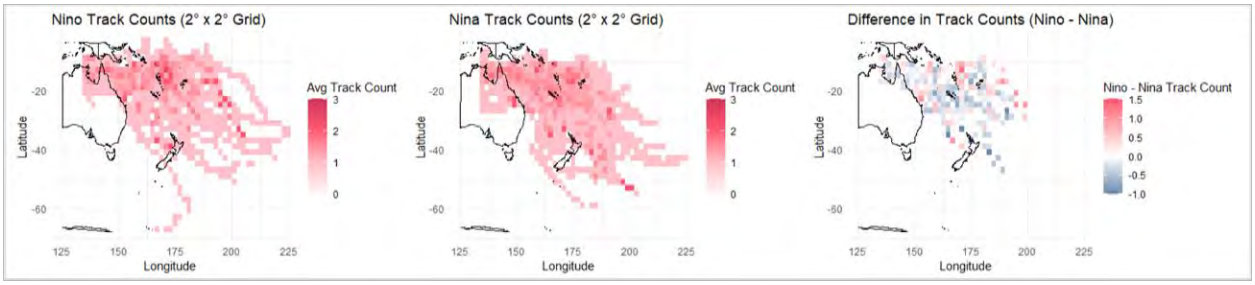


South Indian

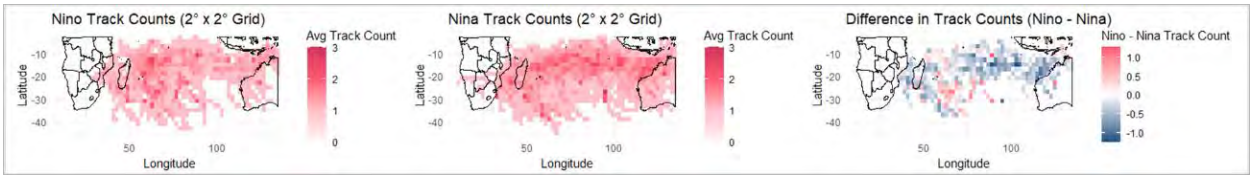


Note: The above figures show the average number of tracks per grid cells (2° x 2°) during El Niño years, La Niña years and the differences between El Niño and La Niña counts, between 1982 and 2023.

## 4.3 CORRELATION MATRIX

The correlation matrix in Figure 4.10 displays the correlation coefficients for each pair of tropical cyclone metrics and climate modulators over the North Hemisphere (upper panel) and South Hemisphere (lower panel). The most significant correlation results are displayed (p-value < 0.05).

Over the West Pacific basin (WP), the strongest positive correlation occurs between the Niño 3.4 index and the average ACE (coefficient = 0.79) and between the Niño 3.4 index and the total tropical cyclone count (0.57). A significant correlation (-0.48) also occurs between the total tropical cyclone count and the AMO. This relationship has been highlighted in previous studies (Sun et al., 2017; Zhang et al., 2018; Huang et al., 2023) that describes the impact of the AMO on the tropical Pacific Ocean surface temperature and atmospheric circulation that could influence the Pacific Ocean tropical cyclone activity.
Over the East Pacific basin (EP), the only significant positive correlation occurs between the Niño 3.4 index and the total tropical cyclone count (coefficient = 0.36). The most significant correlation occurs between the AMO and the ACE (-0.38), which is not expected as the AMO index is computed from the North Atlantic sea surface temperature anomalies and not directly the North Pacific (see West Pacific basin discussion).
Over the North Atlantic basin (NA), the strongest positive correlation occurs between the AMO and the total tropical cyclone count (0.56). The correlation between AMO and the ACE is also significant (0.34). This correlation is expected as a positive AMO means warmer sea surface temperatures over the tropical cyclone development region. The Niño 3.4 index is negatively correlated with the tropical cyclone frequency (-0.48) and intensity (-0.35) in the North Atlantic.
Over the North Indian basin (NI), there is no significant correlation with the tropical cyclone activity to either Niño 3.4 or the AMO. Further research could investigate the influence that other climate modulators, such as the subtropical Indian Ocean Dipole, have on the tropical cyclone activity over the Indian Ocean.

Over the Southern hemisphere, the tropical cyclone activity does not appear to be correlated to the AMO.
The **South Pacific** basin (SP) is positively correlated with the Niño 3.4 index (0.48 for the frequency and 0.46 for the ACE).
The **South Indian** basin (SI) tropical cyclone count is negatively correlated to the Niño 3.4 index (-0.35). This could be due to the rise in sea surface temperature in the central and eastern Pacific during an El Niño event that modifies the Walker circulation, leading to a high-pressure anomaly over part of the South Indian Ocean (Ho et al., 2006).

**Figure 4.10**

CORRELATION MATRIX BETWEEN TROPICAL CYCLONE COUNTS PER BASIN AND CLIMATE MODULATORS OVER BOTH HEMISPHERES

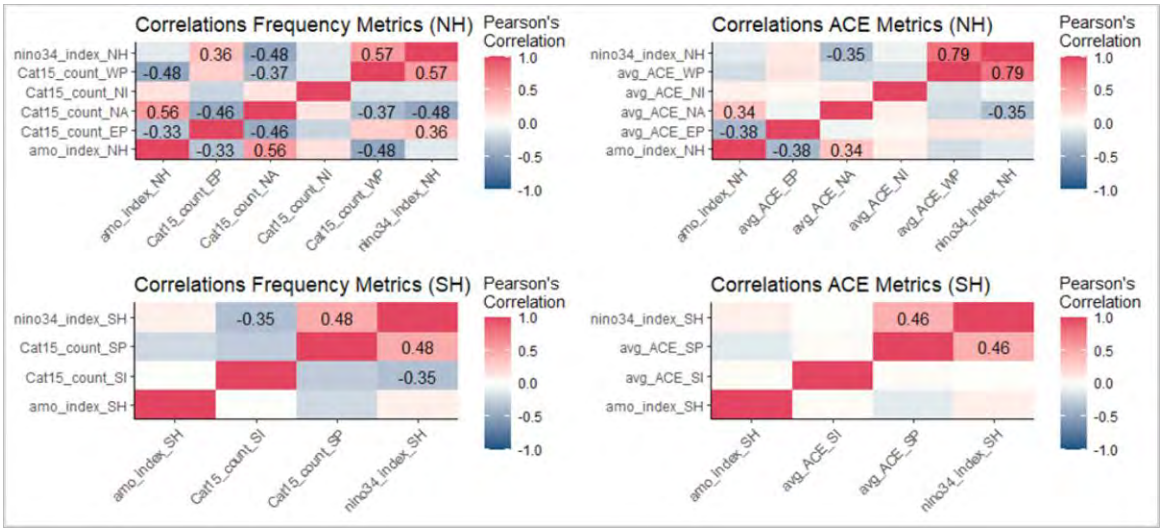


Credit: Correlation matrix plots inspired by https://www.khstats.com/blog/corr-plots/

Figure 4.10 shows the correlations between tropical cyclone metrics (frequency of tropical cyclones of Category 1 to 5 and ACE) and climate modulators (Niño 3.4 index and AMO index) over the North Hemisphere (NH, first row) and South Hemisphere (SH, second row). (EP = East Pacific, NA = North Atlantic, NI = North Indian, SI = South Indian, SP = South Pacific, WP = West Pacific).

## Section 5: Looking Forward – Climate Change Effects on Compound Events

This section explores how climate drivers, i.e., positive temperature anomaly, drought (SPI-6-month), and modulators, i.e., ENSO/ AMO, are impacted by climate change.

*Impact of climate change on compounding positive temperature anomaly and drought*

We computed the SPI-6-month and standardized temperature anomaly for the projection data using the historic timeframe, which allows a direct comparison of climate models from the historic to 2050.

Figure 5.1

CHANGE OF DISTRIBUTION FOR SPI-6-MONTH (DROUGHT) FROM HISTORIC (BLUE) TO 2050 (RED) ACROSS 6 CLIMATE MODELS

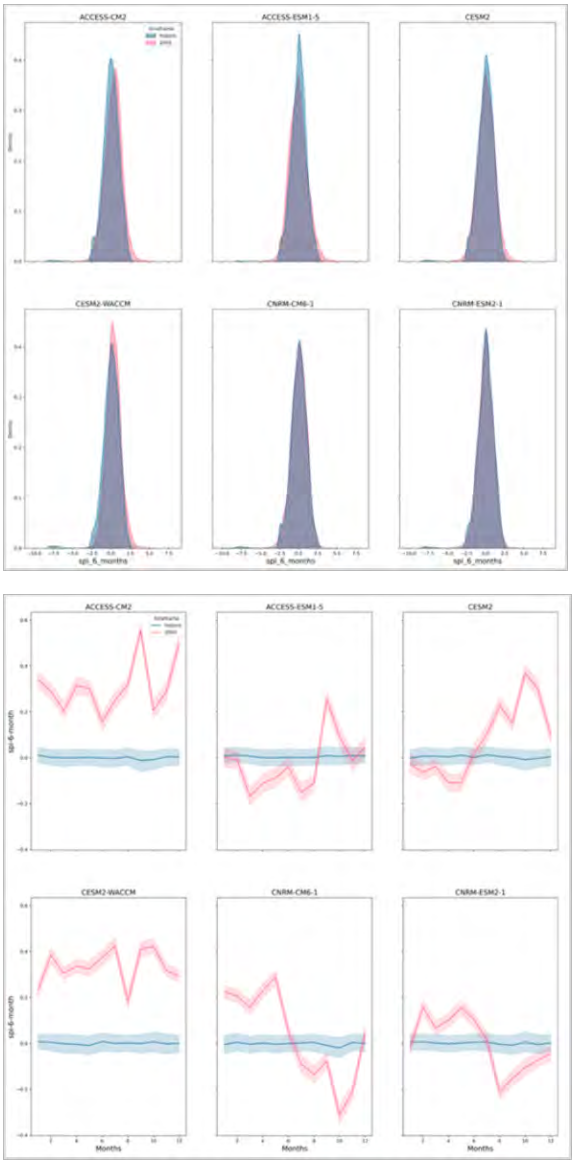

In Figure 5.1, the first graph displays the change in distribution for SPI-6-month from the historic (blue) to 2050 (red), which does not show a strong shift in distribution overall on any model. Looking at the second graph, which provides the timeseries of SPI-6-month, while differences are observed between models, there is no overall trend distinguishable from the graphs. It is important to keep in mind that, even with ACCES-CM2 and CESM2-WACCM models, the variances we observe are within a 0.5 standard deviation from the mean (at best half of the shift we observe for temperature), which still suggests little change as the graph on the left shows.

Figure 5.2

STANDARDIZED TEMPERATURE ANOMALY FROM HISTORIC (BLUE) TO 2050 (RED) ACROSS 6 CLIMATE MODELS

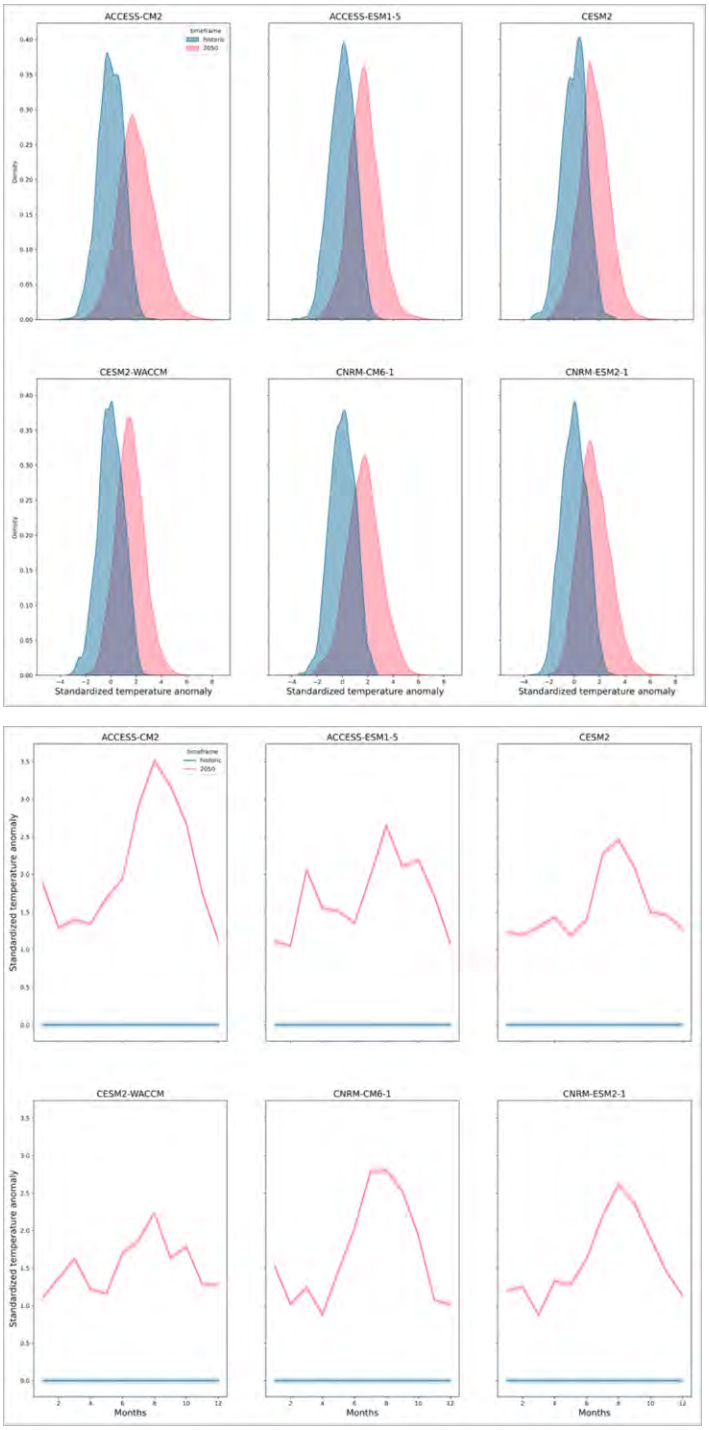





Same plots in Figure 5.2 for standardized temperature anomaly, where it is observed from the first graph a noticeable right shift in the future compared to historic. In the second graph, the trend converges among the models where we notice an overall temperature increase along the year and a spike in July-August.

Figure 5.3

JOINT PLOT OF SPI-6-MONTH (DROUGHT) AND STANDARDIZED TEMPERATURE ANOMALY BASED ON SINGLE CLIMATE MODEL ACCESS-CM2

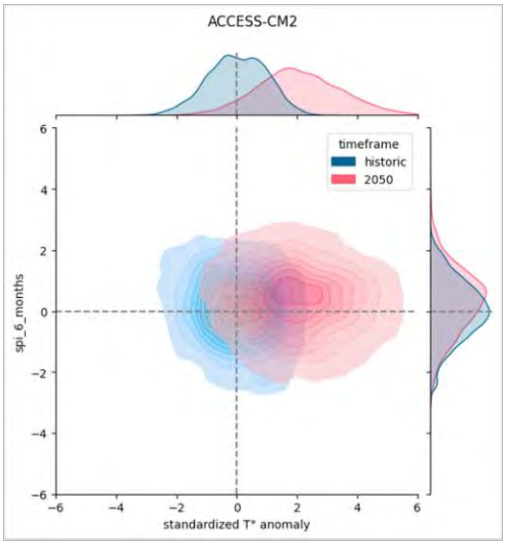


Note: The figure above displays the joint plot of SPI-6-month (drought) and standardized temperature anomaly from the historic (blue) to 2050 (red), based on the single climate model ACCESS-CM2.

A combined view with the two indicators crossed into a joint plot in Figure 5.3 (selected from the ACCESS-CM2 model for illustration purposes; other models show similar distributions) is also presented to illustrate the joint shift from the historic to the 2050 period.

We also computed the probability of having compound events and single events (i.e., positive temperature anomaly or drought) for the historic (baseline) and 2050.

Figure 5.4

MEDIAN TIMESERIES PROBABILITY OF HAVING COMPOUND EVENTS AND SINGLE EVENTS

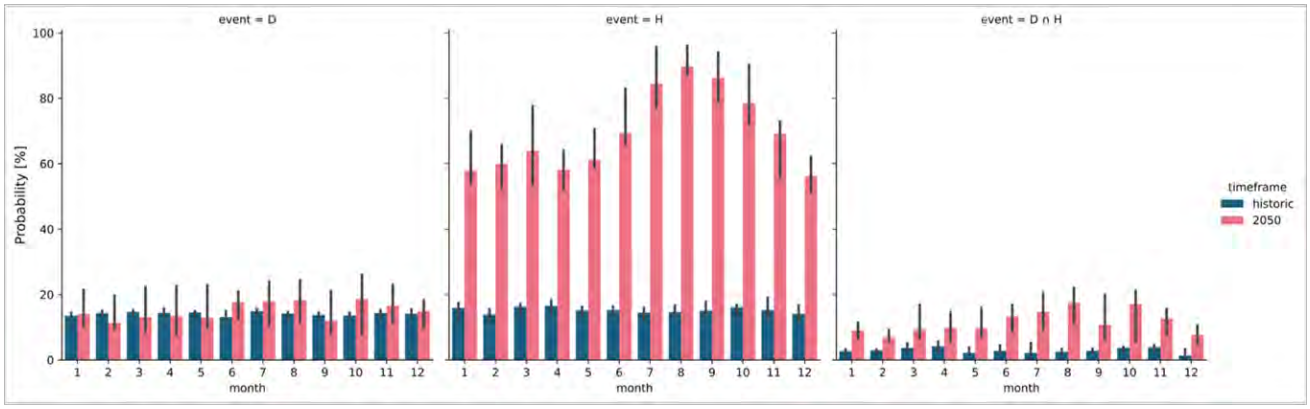


Note: The figure above displays the median timeseries probability of having compound events (left chart) and single events (middle and right charts).The error bars show the dispersion among the models.

The overall probability change is consistent with the distribution shown above, where there is a huge increase in positive temperature anomaly events in the future and little change in drought events. As a result, there is at least a two-fold increase of compound event risk during the year.

Figure 5.5
MEDIAN TIMESERIES PROBABILITY OF HAVING COMPOUND EVENTS AND SINGLE EVENTS

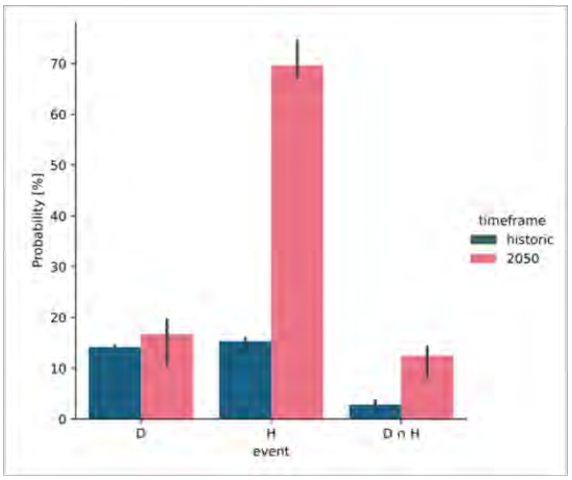


Overall, using the median of the models to study the probability of having compound events between the historic and 2050, there is a 9%-point increase in compound event risks (Future: 12% vs Historic: 3%), whereas there is a 54%-point increase and 3%-point increase in single events of positive temperature anomaly and drought risks, respectively.

*Impact of climate change on ENSO, AMO and tropical cyclones*

Climate modulators, like ENSO and the AMO, could be impacted by climate change, but the nature and extent of these impacts are complex and still subject to ongoing research from the scientific community. Indeed, climate models have limitations in accurately simulating ENSO/ AMO dynamics and their response to climate change.

Climate change impacts the El Niño-Southern Oscillation (ENSO) by potentially increasing the intensity and frequency of its phases, with more pronounced swings between El Niño and La Niña events. Recent research by Cai et al. (2023) suggests that rising greenhouse gas concentrations may have already amplified ENSO variability by up to 10% since 1960, making strong events more extreme and frequent. These changes lead to more severe ENSO-related impacts, such as intensified droughts, floods, heatwaves, and storms. Future projections indicate that if greenhouse gas levels continue to rise, ENSO variations could become even stronger, amplifying its influence on global climate patterns (Rifai et al., 2019). In that vein, the latest IPCC report (WGI, Chp4, 2021) states that the rainfall variability associated with ENSO will intensify.

Regarding AMO, climate models show uncertainties in simulating the AMO and predicting its future behavior under climate change scenarios. This is partly due to the complexity of ice-ocean-atmosphere interactions. A recent study by Mann et al. (2021) has demonstrated that the AMO could have been driven by volcanic activity instead of internally generated by our climate system. The IPCC report (WGI, Chp3, 2021) explains that external forcings, particularly anthropogenic and volcanic aerosols, have influenced the Atlantic Multidecadal Variability, although there is low confidence in the magnitude of this impact due to limitations in model performance and observational data. The general warming of the global oceans due to climate change can influence the SSTs associated with the AMO. This warming can potentially amplify the warm phases of the AMO, leading to more prolonged and intense warm periods. Conversely, increased melting of Arctic sea ice and the influx of fresh, cold water into the North Atlantic can potentially influence the AMO's cold phases. This freshening can affect ocean circulation patterns that influences the AMO.

Climate change influences tropical cyclone activity, and this topic is a focus of active research aimed at understanding the underlying mechanisms and predicting future trends. There is a strong consensus on the increase in tropical cyclone intensity related to warmer ocean temperatures that lead to stronger and more destructive events. The evolution of the frequency of these events is more uncertain, with studies suggesting a global decrease in frequency, but an increase in the proportion of very intense tropical cyclones (IPCC AR6 WG1 chapter 11, 2021; Knutson et al., 2010; Knuston et al., 2020). As the atmosphere warms, its water vapor holding capacity increases (Clausius-Clapeyron relation) leading to more intense precipitation and, as the sea level rises, storm surges will lead to more extensive flooding.

*Impacts from compound events under a warmer climate*

While in this study future climate projections have been thoroughly analyzed, projecting the impacts from compound events has been more challenging. Indeed, projecting the impact of compound events on hazard requires the use of complex mechanical models (wildfire and crop model), which is beyond the scope of this study. Hence, a qualitative approach has been taken to shed some light on how climate change affects the impacts.

For wildfires, as there is a big increase in positive temperature anomaly, in general, and even more in the July-November time period, we can expect a longer wildfire season in the western U.S. that would start earlier, intensify in the summer compared to historic, but also last longer in autumn.

For crop yield, it is not as evident for several reasons. Against rising temperatures, farmers are likely to adapt their agricultural practices by e.g., i) adopting an avoidance strategy by planting crops earlier or later in the season so that the most fragile phenological stage happens at the most suitable moment; ii) switching the crop, though it is a complex decision given the numerous stakes in place, such as market interest, climate suitability, insurance and government subsidies, knowledge, etc.; iii) attempt to grow more robust varieties of the same plant with desired traits, such as heat stress tolerance or a longer/shorter cycle to avoid the effects posed by climate change; and/or iv) increase irrigation against drought; however, if irrigation comes from non-renewable aquifers, adapting by irrigation might not be possible with the end of water availability.

## Section 6: Conclusion and Future Research

This research study aims to understand the different types of compound events and their impacts when events are compounded. Three types of compound events, temporally compounding events, multivariate compounding events, and spatially compounding events, are each studied and analyzed to better quantify and qualify their impacts and trends.

Our study demonstrates that temporally compounding and multivariate compounding drought and heatwave events lead to higher impacts on wildfire or yield loss compared to a single event. Moreover, in the case of yield loss, the intensity of the loss is also higher in the context of compound events. On the other hand, spatially compounding hazards, such as tropical cyclones, can result in multiple regions being impacted at the same time if they are correlated to a same climate driver, potentially increasing annual losses across a portfolio. Conversely, if the hazard across different regions is not correlated to a single climate driver, it can have a balancing effect on the portfolio, reducing overall risk.

As compound events continue to evolve and be researched on, it will become increasingly important to monitor and consider in risk models and analyses, e.g., actuaries and catastrophe modelers, in order to provide more comprehensive and accurate risk assessments, develop better-tailored insurance products and pricing strategies, enhance portfolio management and reinsurance decisions and, ultimately, support more effective disaster preparedness and mitigation efforts.

Building on this work, further research can be done to establish a more robust and holistic understanding of compound events. As we have selected drought and positive temperature anomaly to study, another pair of compounding events or hazards can also be further studied, e.g. cold and wet events, which contribute to high yield losses from multivariate event analysis, in order to gather a more diverse perspective. Similarly, other depending factors that influence the intensity of impacts from compound events could also be introduced for a more robust view. Besides using climate projections of atmospheric variables (e.g., temperature, precipitation, etc.) as input to study impacts (e.g., crop yield and wildfires), physical models can also enable a more quantitative analysis of how future climate compound events will affect the impacts studied.

## Section 7: Acknowledgements

The authors' deepest gratitude goes to those without whose efforts this project could not have come to fruition: the volunteers who generously shared their wisdom, insights, advice, guidance, and arm's-length review of this study prior to publication. Any opinions expressed may not reflect their opinions nor those of their employers. Any errors belong to the authors alone.

Project Oversight Group members:

Joan Barrett, FSA

Timothy Cheng, ASA

Sara Goldberg, FSA

Sam Gutterman, FSA

Priya Rohatgi, ASA

Aadit Sheth, FSA

Peter Sousounis, PhD

At the Society of Actuaries Research Institute:

Rob Montgomery, ASA, Consultant - Research Project Manager

From Axa Climate :

Sophie Abramian, PhD

From Columbia University :

Adam Sobel, PhD

# Appendix

## A.1 DATA

*Temporally compounding and multivariate compounding events (types 1 & 2)*

Climatic drivers – Historical temperature and precipitation used to define temperature anomalies and drought were downloaded from ERA5 (Hersbach, 2023), a product from the European Centre for Medium-Range Weather Forecasts (ECMWF), which provides reanalysis from 1940 to the present.

The resolution in time and space of the data downloaded are 25km and month, respectively. We consider the state of California in the western U.S. as defined in the map below.

Figure A
DEFINITION OF THE GEOGRAPHICAL ZONE (IN RED) WHERE DATA ARE CONSIDERED

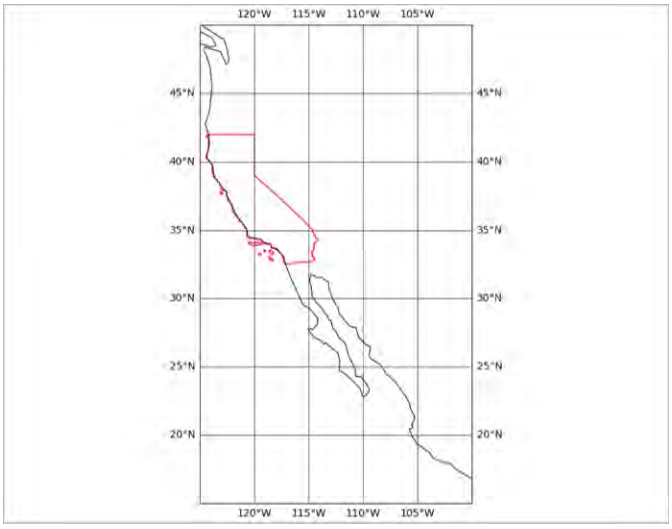


Hazards data:

Wildfires - Data from Monitoring Trend in Burn Severity (MTBS, 2022) are used, which is an interagency program whose goal is to consistently map the burn severity and extent of large fires across all lands of the United States from 1984 to the present. This includes all fires of 1000 acres or greater in the western United States and 500 acres or greater in the eastern Unites States. The extent of coverage includes the continental U.S., Alaska, Hawaii, and Puerto Rico, and we focused our analysis based on the one reported in California.

Crop yield – We used the winter wheat data from the United-States Department of Agriculture (USDA) in California that are available from 1950 to 2022 at the county level. The data has an increasing trend, which comes from a mix of technological improvement and climate change. As the technological improvement trend cannot be disaggregated from the data source, the 2005–2022-time window is specifically selected as it shows minimal technological-influenced trends. For the rest of the analysis, we continue with2005–2022-time window.

*Spatially compounding events (type 3)*

The International Best Track Archive for Climate Stewardship (IBTrACS) database is used to assess the spatially compounding tropical cyclones. It includes tropical cyclone characteristics such as their intensity, location and time from various meteorological agencies worldwide (Gahtan *et al.*, 2024; Knapp *et al.*, 2010). The climatology of the number of tropical cyclones worldwide shows an evolution of the number of events at the start of the satellite era in the 1980s. Therefore, we concentrated this study on the period ranging from 1980 to 2023 to remove this observational bias.

The AMO monthly dataset (Enfield et al., 2001) was provided by the NOAA PSL, Boulder, Colorado, USA, from their website at https://psl.noaa.gov/data/timeseries/AMO/. The retrieved data is the AMO unsmoothed long record. The ENSO monthly dataset is the OISST.v2.1 provided by the NOAA CPC website at https://www.cpc.ncep.noaa.gov/data/indices/sstoi.indices. It is the Niño 3.4 index, which is the SST anomaly averaged over 5°N-5°S and 170-120°W.

*Future climate*

Future projected temperature and precipitation were extracted for the baseline (1985-2014) and 2050 period (2035-2065) over the same region (California). We used six downscaled climate models that are open source and freely available for download (Thrasher, B., 2021; Thrasher, B., 2022):

- ACCESS-CM2
- ACCESS-ESM1-5
- CESM2
- CESM2-WACCM
- CNRM-CM6-1
- CNRM-ESM2-1

Models have a daily time resolution and spatial resolution of one degree.

Data from the 2050 period are projections following the SSP5-8.5 emissions scenario and climate forcing elements. "SSP5" refers to Shared Socioeconomic Pathway 5, which describes a world of rapid economic growth, technological progress, and fossil fuel-intensive development (IPCC, 2022). This pathway is characterized by a few factors: i) low population growth, ii) very high economic growth, iii) high energy demand, iv) fossil fuel-dominated energy systems, and v) low challenges to adaptation but high challenges to mitigation.

The "8.5" indicates a radiative forcing level of 8.5 W/m² by 2100. This high forcing results from: i) very high greenhouse gas emissions, ii) approximately 6.5 times more coal use in 2100 compared to today, and iii) $CO_2$ emissions about 20% higher than the original RCP8.5 scenario by the century's end.

SSP5-8.5 represents the upper end of the scenario spectrum, intended as a high-emissions reference case rather than the most likely "business as usual" outcome. It's useful for exploring potential worst-case climate impacts but should not be considered the default future pathway.

## A.2 METHODOLOGY

*Temporally compounding events (type 1)*

The methodology consisted of associating any wildfire with the environmental condition in term of heat and drought where they exist. For each wildfire, we have access to the temperature anomaly (see below) at its specific location the day it happens and, in the same manner, access to the drought index (see below) at that time and location. As described in the previous section, our climatic data are monthly, and a wildfire can last from one day to one month, so we only considered the initial condition of the fire i.e., the day it started.

*Temperature anomaly and drought metrics*

Temperature anomaly - This refers to a deviation from a long-term average temperature. These anomalies can be positive (warmer than average) or negative (cooler than average) and are used to monitor and understand climate variations and trends.

We used standardized temperature anomaly as the temperature indicator and a heat event is any month where the standardized temperature is above one standard deviation from the mean. Rather than looking into the difference between the monthly temperature and the long-term average temperature for a specific month, standardized temperature anomaly relies on the dispersion of data and allows the capture of extreme events without using any physical threshold.

To illustrate what constitutes a temperature anomaly in the western U.S., Figure B below shows the climatology of each month from 1950 to 2023, with temperature measured every month.

Figure B

MONTHLY MEAN TEMPERATURE IN WESTERN U.S. FROM 1950 TO 2023

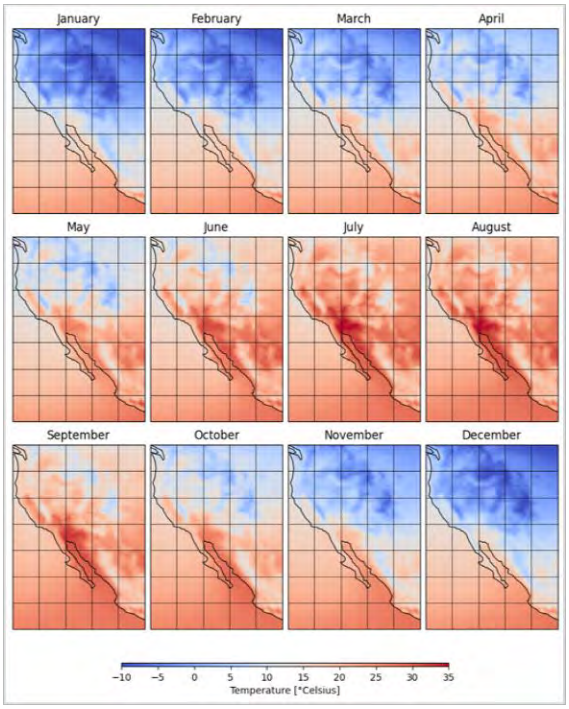

We computed temperature anomaly by measuring the discrepancy between the monthly average measured temperature and average temperature for the given month over the period (displayed in Figure C below), written as:

$$T'(lat, lon, month) = \frac{T(lat, lon, month) - \bar{T}(lat, lon, month)}{\sigma_T(lat, lon, month)}$$

where T' denotes the standardized anomaly, and is defined along the whole time series, T is the measured temperature at each timestep, $\bar{T}(lat, lon, month)$ the month average over 1950 to 2023, and $\sigma(lat, lon, month)$ the month standard deviation over 1950 to 2023.

Thus, we could examine a particular month and quantify, for any region in the western U.S., the temperature anomaly, as shown in Figure C below.

Figure C

TEMPERATURE ANOMALY CALCULATED ON AUGUST 1950

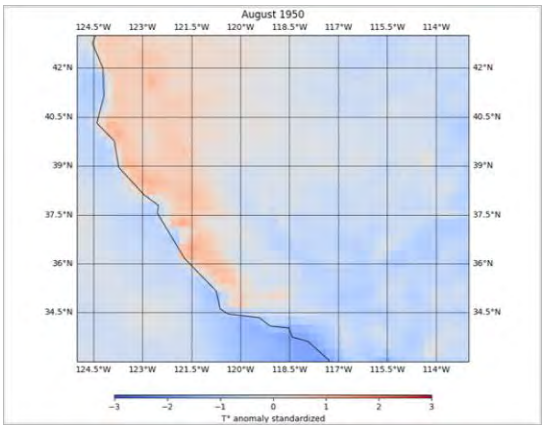


**Drought -** The IPCC Sixth Assessment Report defines a drought simply as "drier than normal conditions." This implies that a drought is "a moisture deficit relative to the average water availability at a given location and season." According to the National Integrated Drought Information System, a multi-agency partnership, a drought is generally defined as "a deficiency of precipitation over an extended period of time (usually a season or more), resulting in a water shortage."

Drought, a complex phenomenon related to the absence of water, is challenging to monitor and define. By the early 1980s, over 150 definitions of "drought" had already been published. The range of definitions reflects differences in regions, needs, and disciplinary approaches.

There are three major categories of drought based on where in the water cycle the moisture deficit occurs: meteorological drought, hydrological drought, and agricultural or ecological drought. This research only focused on meteorological drought, which occurs due to a lack of precipitation and usually precedes the other kinds of drought. As a drought persists, the conditions surrounding it gradually worsen, and its impact on the local population gradually increases.

The Standardized Precipitation Index (SPI) and Standardized Precipitation Evapotranspiration Index (SPEI) are widely used indices to characterize meteorological drought on a range of timescales. SPI was used for the purpose of this study instead of SPEI as SPEI integrates temperature in its computation, which overlaps with our research effort to be already looking at temperature with the positive temperature anomaly indicator. The SPI quantifies observed precipitation as a standardized departure from a selected probability

distribution function that models the raw precipitation data. The SPI values can be interpreted as the number of standard deviations by which the observed anomaly deviates from the long-term mean.

**Figure D**

METHODOLOGY OF STANDARDIZED PRECIPITATION INDEX COMPUTATION

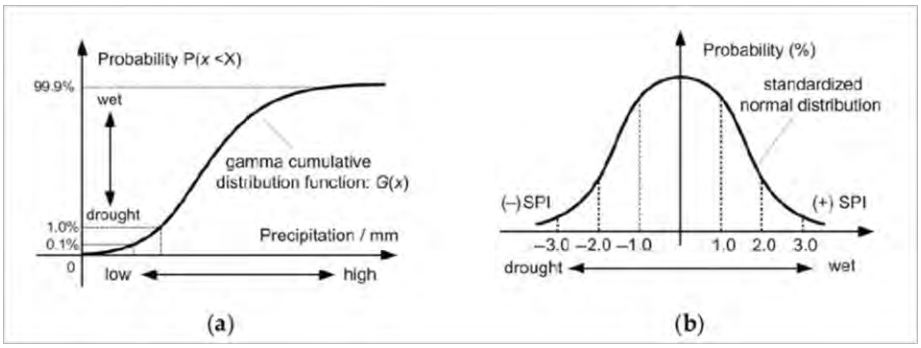


Credit: Sakellariou, et al. (2024). Spatiotemporal Drought Assessment Based on Gridded Standardized Precipitation Index (SPI) in Vulnerable Agroecosystems. Sustainability. 16. 10.3390/su16031240.

Note: Figure D displays the normalized distribution applied by the SPI: (a) fitted gamma distribution for the cumulated monthly precipitation and (b) standardized normal distribution for SPI. Wetness (positive SPI)/dryness (negative SPI)

We computed the SPI index from 1950 to 2023 with a six-month period of accumulated precipitation and standardized it over the period from 1980 to 2023, with a four-step computation process: 1) cumulative precipitations were computed using a rolling-window where the width depends on the need (from 1 month to 36 months); 2) precipitation data were fitted to a gamma probability density function, which works better than the other probability density functions such as Weibull or log-normal; 3) results were used to find the cumulative probability of a precipitation event for a given month and time scale; and 4) the cumulative probability distribution was transformed into a standard normal distribution, with a mean of zero and variance of one, which is the SPI value (Cheval, S., 2015).

**Figure E**

DROUGHT INDEX CALCULATED ON AUGUST 1950

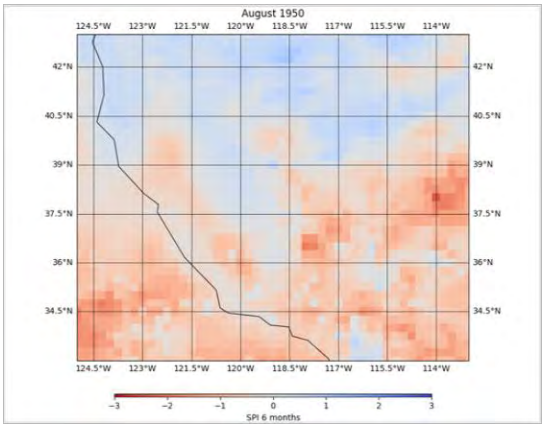


Thus, we could examine a particular month and quantify, for any region in the western U.S., the drought, as shown in Figure E above.

Once the drought and temperature anomaly context were computed for each wildfire, we displayed the different conditions in which they happened in a phase diagram, with the x-axis temperature anomaly and the y-axis the drought index presented with interpretation per quadrant as follows:

**Figure F**

PHASE DIAGRAM FOR COMPOUND WEATHER EVENTS ASSESSMENT

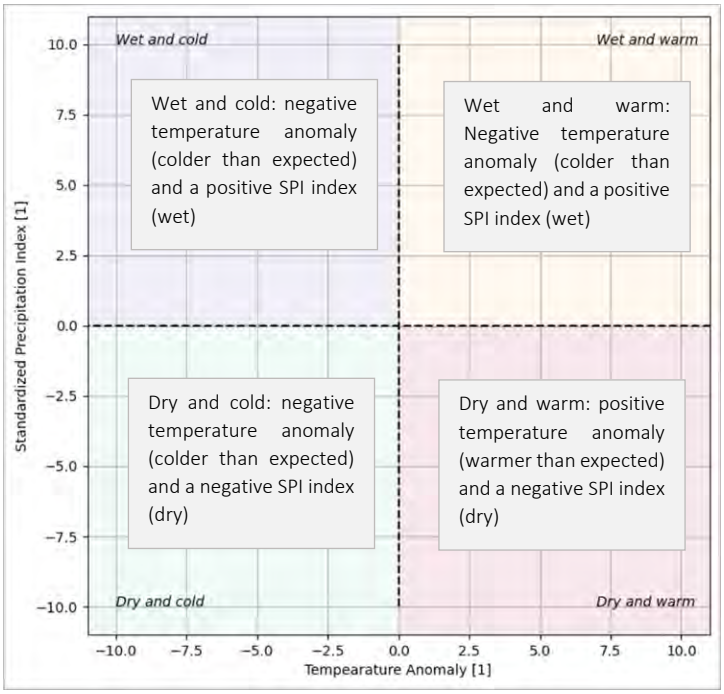


Note: The bottom right quadrant is compound drought and positive temperature anomaly and is the focus of our study.

Then, we continued the analysis by quantifying the frequency of the wildfires under single events (drought and positive temperature anomaly ) and type 1 compound events ( positive temperature anomaly preceding drought ).

*Multivariate compounding events (type 2)*

The methodology consisted in associating crop yield with the environmental condition in terms of heat and drought at the county scale. The time window during which we looked at the environmental condition with regards to the yield was the flowering period. To compare yields across time and space, we focused only on a subset of the data (2005-2022) without a trend and standardized the yield. Then, we studied in which conditions yield loss (i.e, standardized yield < 0 ) happened.

We used the same phase diagram from Figure F and focused the further analysis on the bottom right quadrant. We evaluated the effect of type 2 compound events on crop yield both in terms of frequency (i.e., the probability of having a yield loss) and intensity (i.e., the size of the yield loss).

We elaborate in further detail in subsection 3.1.

*Spatially compounding events (type 3)*

The analysis was performed over the following six tropical cyclone basins as defined within the Ibtracs technical documentation (2024,) where most of the tropical cyclone activity occurs (Figure G). The South Atlantic Ocean has only seen one event reaching tropical cyclone strength (intensity of at least 64 knots) since the 1970s so it was not considered in this study.

Northern Hemisphere basins:

- NI = North Indian: 30° < Longitude < 100°
- WP = Western Pacific: 100° < Longitude < 180°
- EP = Eastern Pacific: Western Boundary = 180°; Eastern Boundary = Coastline of North America on the North Atlantic
- NA = North Atlantic: Western Boundary = Coastline of North America on the Eastern Pacific; Eastern Boundary = 30°

Southern Hemisphere basins:

- SI = South Indian: 10° < Longitude < 135°
- SP = South Pacific: 135° < Longitude < 290°
- SA = South Atlantic -70° < Longitude < 10°

Figure G

*TROPICAL CYCLONE BASINS' LOCATION AND NAMES*

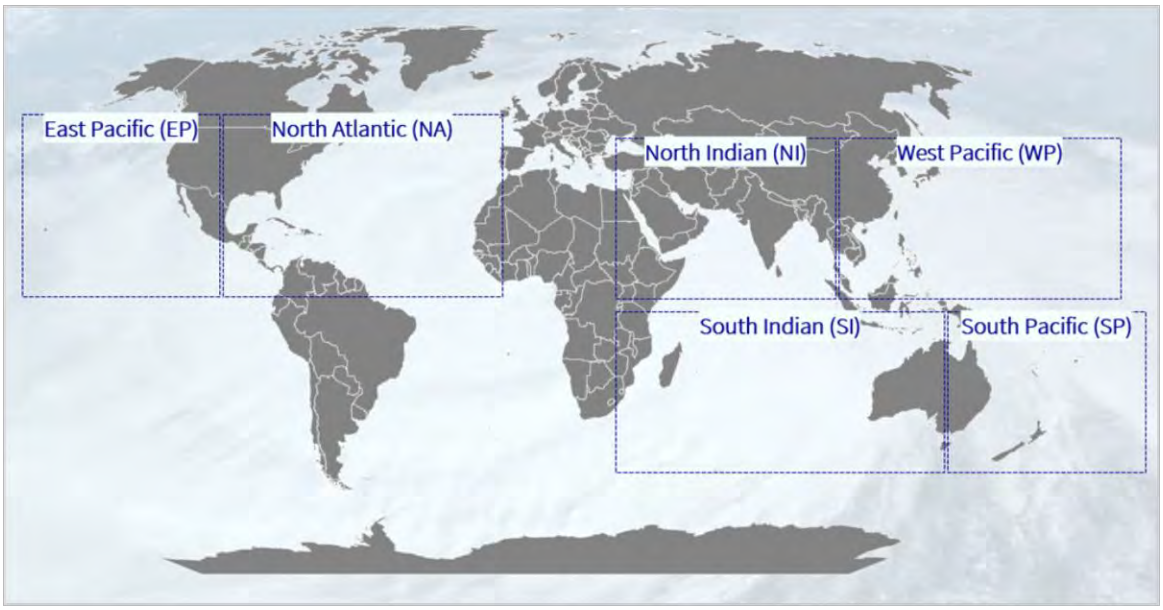

*Tropical cyclone metrics*

A variety of metrics can be used to quantify the severity of a tropical cyclone season. These metrics represent the intensity and frequency of tropical cyclones and are influenced by climate drivers.

- The intensity of tropical cyclone season was studied using the Accumulated Cyclone Energy (ACE) metric. It is calculated by summing the squares of the estimated maximum sustained wind speeds of each storm (in knots) at six-hour intervals while the storms are at least tropical storm strength.
- The frequency of the tropical cyclone season was evaluated through the number of tropical cyclones. We distinguished between all tropical cyclones (category 1 and above on the Saffir-Simpson hurricane wind scale) and very intense tropical cyclones (category 3 and above on the Saffir-Simpson hurricane wind scale).
- The spatial distribution of the tropical cyclone activity was studied by computing:
    - The total number of tracks considering all events regardless of their intensities between 1982 and 2023
    - The average latitude of the maximum windspeed along each track

*Climate drivers*

Climate drivers impact tropical cyclone activity though their influence from key environmental factors such as sea surface temperatures, vertical wind shear, and atmospheric stability, which are critical for tropical cyclone development and intensity. The two most significant are El Nino Southern Oscillation (ENSO) and the Atlantic Multidecadal Oscillation (AMO).

*El Niño-Southern Oscillation (ENSO):* ENSO is a long-term fluctuation in Pacific Ocean sea surface temperatures and atmospheric conditions, typically lasting several months to a few years.

- *El Niño*: This phase is characterized by warmer-than-average sea surface temperatures in the central and eastern Pacific Ocean. El Niño typically reduces Atlantic hurricane activity due to increased vertical wind shear and stable atmospheric conditions. Conversely, it can enhance cyclone activity in the central and eastern Pacific.
- *La Niña*: This phase features cooler-than-average sea surface temperatures in the central and eastern Pacific. La Niña generally increases Atlantic hurricane activity by reducing vertical wind shear and creating more favorable atmospheric conditions. It can decrease cyclone activity in the central and eastern Pacific.
- *Neutral phase*: During this phase, sea surface temperatures (SSTs) in the central and eastern Pacific are close to the long-term average, without significant warming or cooling trends. Tropical cyclone activity tends to be near the climatological average.

The ENSO index is derived over the Niño 3.4 region (5°N-5°S, 120°W-170°W), which can capture both El Niño and La Niña phases more comprehensively and influence global atmospheric circulation patterns impacting tropical cyclone activity worldwide.

*Atlantic Multidecadal Oscillation (AMO):* The AMO is a long-term fluctuation in North Atlantic sea surface temperatures, typically lasting several decades.

- Warm Phase: During the warm phase, sea surface temperatures in the North Atlantic are above average, leading to increased hurricane activity. Warmer waters provide more energy for storm formation and intensification.
- Cool Phase: During the cool phase, sea surface temperatures are below average, resulting in decreased hurricane activity. Cooler waters provide less energy, leading to fewer and weaker storms.

*Future climate*

The study focused on the same California region for the type 1 and type 2 sections. The methodology consisted of analyzing the evolution of temperature anomaly, SPI-6-month and their joint distribution at the model level. Afterwards, we quantified the evolution of single events and multivariate compound events (type 2) from baseline to the 2050 period.

## A.3 LIMITATIONS

*Temporal compounding event – type 1*

When studying temporal compound event effects on wildfires, we used monthly weather data that didn't allow us to capture short-term variations that are important when studying wildfire intensity such as wind speed.

In addition, we did not explore the climate drivers that lead to the co-occurrence of the hazards, for instance blocking patterns, and why they could happen more frequently.

*Multivariate compounding events – type 2*

We focused our research on the flowering period as it is the period during which the crop yield is the most sensible. It happens around two months before harvest.  We overlooked the effect of compound events on the rest of the crop cycle.

Moreover, only dry and hot weather were considered for crop loss, although wet and cold weather can be as detrimental to crop yield.

*Spatially Compounding – type 3*

Climate drivers and tropical cyclone activity monitoring relies on observations which are limited in time. Analyzing the AMO index starting as early as 1950 or 1900 would capture one or two complete cycles of both positive and negative AMO phases and, therefore, enhance the robustness of the conclusions.

In addition, the study focused on the analysis of correlations between climate drivers and hazards (tropical cyclone metrics) but did not investigate further how they dynamically interact, which would require the use of climate models.

*Future climate*

To further investigate the evolution of compounding climate hazards, we recommend an analysis of a larger number of models and different climate emission scenarios (e.g. SSP2-4.5, SSP3-7.0 among others) and time periods (e.g. 2070, 2100).

## References

Bevacqua, E., Suarez-Gutierrez, L., Jézéquel, A., Lehner, F., Vrac, M., Yiou, P., & Zscheischler, J. (2023). Advancing research on compound weather and climate events via large ensemble model simulations. *Nature communications*, *14*(1), 2145. https://doi.org/10.1038/s41467-023-37847-5

Cai, W., Ng, B., Geng, T. *et al.* (2023). Anthropogenic impacts on twentieth-century ENSO variability changes. *Nat Rev Earth Environ* 4, 407–418. https://doi.org/10.1038/s43017-023-00427-8

Cheval, S. (2015). The standardized precipitation index – an overview. *Romanian Journal of Meteorology, 12*, 17-64.

Enfield, D.B., A.M. Mestas-Nunez, and P.J. Trimble. (2001). The Atlantic Multidecadal Oscillation and its relationship to rainfall and river flows in the continental U.S. *Geophys. Res. Lett.*, 28: 2077-2080.

Fuhrer, J., Beniston, M., Fischlin, A., Frei, C., Goyette, S., Jasper, K., & Pfister, C. (2006). Climate risks and their impact on agriculture and forests in Switzerland. *Climatic Change, 79*(1-2), 79-102. https://doi.org/10.1007/S10584-006-9106-6

Gahtan, J., K. R. Knapp, C. J. Schreck, H. J. Diamond, J. P. Kossin, M. C. Kruk. (2024). International Best Track Archive for Climate Stewardship (IBTrACS) Project, Version 4r01. NOAA National Centers for Environmental Information. doi:10.25921/82ty-9e16

Hersbach, H., Bell, B., Berrisford, P., Biavati, G., Horányi, A., Muñoz Sabater, J., Nicolas, J., Peubey, C., Radu, R., Rozum, I., Schepers, D., Simmons, A., Soci, C., Dee, D., & Thépaut, J.-N. (2023). ERA5 monthly averaged data on single levels from 1940 to present. *Copernicus Climate Change Service (C3S) Climate Data Store (CDS)*. https://doi.org/10.24381/cds.f17050d7

Ho C-H, Kim J-H, Jeong J-H, Kim H-S, Chen D. (2006). Variation of tropical cyclone activity in the South Indian Ocean: El Niño-Southern Oscillation and Madden-Julian Oscillation effects. *Journal of Geophysical Research* **111**: D22101, https://doi.org/10.1029/2006JD007289

Huang, H., Collins, W. D., Patricola, C. M., Ruprich-Robert, Y., Ullrich, P. A., & Baker, A. J. (2023). Contrasting Responses of Atlantic and Pacific Tropical Cyclone Activity to Atlantic Multidecadal Variability. Geophysical Research Letters, 50(10). Portico. https://doi.org/10.1029/2023gl102959

Intergovernmental Panel on Climate Change (IPCC). (2012). *Managing the risks of extreme events and disasters to advance climate change adaptation: A special report of Working Groups I and II of the Intergovernmental Panel on Climate Change* (C. B. Field, V. Barros, T. F. Stocker, D. Qin, D. J. Dokken, K. L. Ebi, M. D. Mastrandrea, K. J. Mach, G.-K. Plattner, S. K. Allen, M. Tignor, & P. M. Midgley, Eds.). Cambridge University Press.

International Best Track Archive for Climate Stewardship (Ibtracs) Technical documentation (2024). https://www.ncei.noaa.gov/sites/g/files/anmtlf171/files/2024-07/IBTrACS_version4r01_Technical_Details.pdf

IPCC, The Physical Science Basis. Contribution of Working Group I to the Sixth Assessment Report of the Intergovernmental Panel on Climate Change. (2021). Summary for Policymakers. *Cambridge University Press*, Cambridge, United Kingdom and New York, NY, USA, pp. 3–32.

IPCC, The Physical Science Basis. Contribution of Working Group I to the Sixth Assessment Report of the Intergovernmental Panel on Climate Change. Chapter 3. (2021). Human Influence on the Climate System. In

Climate Change 2021: The Physical Science Basis. Contribution of Working Group I to the Sixth Assessment Report of the Intergovernmental Panel on Climate Change. *Cambridge University Press*, Cambridge, United Kingdom and New York, NY, USA, pp. 423–552.

IPCC, The Physical Science Basis. Contribution of Working Group I to the Sixth Assessment Report of the Intergovernmental Panel on Climate Change. Chapter 4. (2021). Future Global Climate: Scenario-based projections and near-term information. *Cambridge University Press,* Cambridge, United Kingdom and New York, NY, USA, pp. 553–672.

IPCC, The Physical Science Basis. Contribution of Working Group I to the Sixth Assessment Report of the Intergovernmental Panel on Climate Change. Chapter 11. (2021). Weather and climate extreme events in a changing climate. *Cambridge University Press,* Cambridge, United Kingdom and New York, NY, USA. https://doi.org/10.1017/9781009157896.013

IPCC, Contribution of Working Group II to the Sixth Assessment Report of the Intergovernmental Panel on Climate Change. (2022). Impacts, adaptation, and vulnerability. *Cambridge University Press,* Cambridge, United Kingdom and New York, NY, USA. https://doi.org/10.1017/9781009325844

Knapp, K. R., M. C. Kruk, D. H. Levinson, H. J. Diamond, and C. J. Neumann. (2010). The International Best Track Archive for Climate Stewardship (IBTrACS): Unifying tropical cyclone best track data. *Bulletin of the American Meteorological Society*, 91, 363-376. doi:10.1175/2009BAMS2755.1

Knutson, T., McBride, J., Chan, J. et al. (2010). Tropical cyclones and climate change. *Nature Geosci* 3, 157–163. https://doi.org/10.1038/ngeo779

Knutson TR, Camargo SJ, Chan JCL, Emanuel K, Ho C, Kossin JP, Mohapatra M, Satoh M, Sugi M, Walsh K, Wu L (2020) Tropical cyclones and climate change assessment: part II. Projected response to anthropogenic warming. *Bull Am Meteor Soc* 10. https://doi.org/10.1175/BAMS-D-18-0194.1

Levine, A. F. Z., M. J. McPhaden, and D. M. W. Frierson. (2017). The impact of the AMO on multidecadal ENSO variability, *Geophys. Res. Lett.*, 44, 3877–3886, doi:10.1002/2017GL072524

Mann, M. E., Steinman, B. A., Brouillette, D. J., and Miller, S. K. (2021). Multidecadal climate oscillations during the past millennium driven by volcanic forcing. *Science*, 371, 1014–1019, https://doi.org/10.1126/science.abc5810

Monitoring Trends in Burn Severity. (2022). *Monitoring Trends in Burn Severity*. https://www.mtbs.gov/

Rifai S. W. *et al.* (2019). *Environ. Res. Lett.* 14 105002DOI 10.1088/1748-9326/ab402f

Stott, P. (2016). How climate change affects extreme weather events. *Science, 352*(6293), 1517-1518. https://doi.org/10.1126/science.aaf7271

Sun, C., Kucharski, F., Li, J. *et al.* (2017). Western tropical Pacific multidecadal variability forced by the Atlantic multidecadal oscillation. *Nat Commun* 8, 15998. https://doi.org/10.1038/ncomms15998

Thrasher, B., Wang, W., Michaelis, A. et al. NASA Global Daily Downscaled Projections, CMIP6. Sci Data 9, 262 (2022). https://doi.org/10.1038/s41597-022-01393-4

Thrasher, B., Wang, W., Michaelis, A., Nemani, R. (2021). NEX-GDDP-CMIP6. NASA Center for Climate Simulation. https://doi.org/10.7917/OFSG3345

Tripathy, K., Mukherjee, S., Mishra, A., Mann, M., & Williams, A. (2023). Climate change will accelerate the high-end risk of compound drought and heatwave events. *Proceedings of the National Academy of Sciences of the United States of America, 120*(28), e2219825120. https://doi.org/10.1073/pnas.2219825120

United States Department of Agriculture (USDA). (n.d.). Quick stats. *United States Department of Agriculture*. https://www.nass.usda.gov/Quick_Stats/Lite/index.php

van den Hurk, B. J. J. M., White, C. J., Ramos, A. M., Ward, P. J., Martius, O., Olbert, I., Roscoe, K., Goulart, H. M. D., & Zscheischler, J. (2023). Consideration of compound drivers and impacts in the disaster risk reduction cycle. *iScience*, *26*(3), 106030. https://doi.org/10.1016/j.isci.2023.106030

World Meteorological Organization (WMO). (2014). El Niño/Southern Oscillation (WMO-No. 1145). https://library.wmo.int/records/item/53800-el-nino-southern-oscillation?offset=3

Zhang, W., Vecchi, G. A., Murakami, H., Villarini, G., Delworth, T. L., Yang, X., & Jia, L. (2018). Dominant role of Atlantic multidecadal oscillation in the recent decadal changes in western North Pacific tropical cyclone activity. *Geophysical Research Letters, 45(1), 354–362*. https://doi.org/10.1002/2017GL076397

Zscheischler, J., Martius, O., Westra, S., Bevacqua, E., Raymond, C., Horton, R. M., Seneviratne, S. I., & Vignotto, E. (2020). A typology of compound weather and climate events. *Nature Reviews Earth & Environment, 1*(7), 333-347. https://doi.org/10.1038/s43017-020-0060-z

## About The Society of Actuaries Research Institute

Serving as the research arm of the Society of Actuaries (SOA), the SOA Research Institute provides objective, data-driven research bringing together tried and true practices and future-focused approaches to address societal challenges and your business needs. The Institute provides trusted knowledge, extensive experience and new technologies to help effectively identify, predict and manage risks.

Representing the thousands of actuaries who help conduct critical research, the SOA Research Institute provides clarity and solutions on risks and societal challenges. The Institute connects actuaries, academics, employers, the insurance industry, regulators, research partners, foundations and research institutions, sponsors and non-governmental organizations, building an effective network which provides support, knowledge and expertise regarding the management of risk to benefit the industry and the public.

Managed by experienced actuaries and research experts from a broad range of industries, the SOA Research Institute creates, funds, develops and distributes research to elevate actuaries as leaders in measuring and managing risk. These efforts include studies, essay collections, webcasts, research papers, survey reports, and original research on topics impacting society.

Harnessing its peer-reviewed research, leading-edge technologies, new data tools and innovative practices, the Institute seeks to understand the underlying causes of risk and the possible outcomes. The Institute develops objective research spanning a variety of topics with its strategic research programs: aging and retirement; actuarial innovation and technology; mortality and longevity; diversity, equity and inclusion; health care cost trends; and catastrophe and climate risk. The Institute has a large volume of topical research available, including an expanding collection of international and market-specific research, experience studies, models and timely research.

Society of Actuaries Research Institute
8770 W Bryn Mawr Ave, Suite 1000
Chicago, IL 60631